Title
Excitatory Circuits in a Mouse Model of Type I Lissencephaly

Author
Greenwood, Joel Simeon Fogde

Publication Date
2008-09-10

Peer reviewed|Thesis/dissertation

Excitatory Circuits in a Mouse Model of Type I Lissencephaly

by

Joel Simeon Fogde Greenwood

DISSERTATION

Submitted in partial satisfaction of the requirements for the degree of

DOCTOR OF PHILOSOPHY

in

Neuroscience

in the

GRADUATE DIVISION

of the

UNIVERSITY OF CALIFORNIA, SAN FRANCISCO

Dedication and Acknowledgements

I would like to thank Rosanne "The Brain Snatcher" Estrada who kindly took over the EEG portion of the project (and in fact transplanted and recorded all of the mice presented in Figure 1 of Chapter Two) when it was clear I was not going to have time to finish it. Peter Ohara is here acknowledged, and thus cannot escape or wash his hands of the role he played in teaching me to perform and interpret electron microscopy. I would like to thank Larry Ackerman for letting me run amok with expensive, sensitive equipment. I would also like to thank Josh Taylor and Gregg Whitworth who together lead me down the dark path of computer programming and held my hand (thank you Google chat) when I needed it.

I would like to thank the Berkeley Hang Gliding Club for teaching me perspective and for memories money couldn't buy and life will never take from me.

Finally, I would like to thank best friend and partner in crime, Doctor Wendy Rocket. I am looking forward to a lifetime of adventure with you.

Statement of Contribution

Dr. Yanling Wang performed the lipophilic dye tracing, glutamate receptor staining, and astrocyte staining presented in Chapter One.

Rosanne Estrada performed the EEG study presented in Chapter Two.

Larry Ackerman cut and mounted the ultra thin sections used for electron microscopy presented in Chapter Two.

Excitatory Circuits in a Mouse Model of Type I Lissencephaly

by

Joel Simeon Fogde Greenwood

ABSTRACT

Structural abnormalities in the human brain, which result from disruption of cortical development, are often associated with neurological deficits such as mental retardation and epilepsy. Cortical malformations that result in epilepsy are often resistant to standard antiepileptic drugs leaving the patient with few options for successful treatment. A driving question in the field of epilepsy research is to understand the basis of seizure generation in the malformed brain, in the hope of providing new methods to treat this devastating condition. Lissencephaly in humans is characterized by a lack of cortical gyri and four-layered cortex, and by mental retardation and epilepsy. The Lis1 protein has been shown to interact with the dynein/dynactin complex and to be critical for neuronal migration. A mouse model of lissencephaly was created by heterozygous mutation of the *Lis1* gene. The *Lis1* +/- mutant mouse has neuronal disorganization of the cortex, olfactory bulb, and hippocampus. This mouse has been shown to have hyperexcitability in vitro, impairment of special learning in vivo, and an intact inhibitory system. Fifteen years after the discovery of Lis1's involvement in lissencephaly and ten

years after the development of a mouse model for the disease, the basis of seizure generation remains a mystery. In this thesis I examined the excitatory system of the hippocampus, specifically CA1 pyramidal cells and their synaptic inputs. I found that the glutamatergic system is intact and functioning relatively normally; however, excitatory synaptic input onto CA1 pyramidal cells is nearly doubled in Lis1 +/- mutants. I also showed that the vesicular pool at excitatory synaptic contacts onto CA1 pyramidal cells is enlarged and importantly, the readily releasable pool (RRP) of synaptic vesicles is enlarged. I then examined the consequences of this change and found that Lis1 +/- mutants have enhanced short-term plasticity, which may underlie hyperexcitability and ultimately seizure generation in these mice. Finally, I showed that reducing calcium entry in these terminals eliminates this excitability. These data suggest a molecular basis for seizure generation in the lissencephalic brain and offer a new way to approach treatment for this disease.

Table of Contents

List of Figures

Page

CHAPTER ONE

CHAPTER TWO

CHAPTER ONE

Disruption of Hippocampal Excitatory Circuits in Heterozygous *Lis1* Mutant Mice

ABSTRACT

Lissencephaly-1 (*Lis1*) heterozygotic mice exhibit severe hippocampal disorganization. In humans with *Lis1* haploinsufficiency, abnormal neuronal migration and severe neuronal disorganization contribute to cognitive impairment and seizures early in life. Using a mouse model, we examined the functional impact of *Lis1* deficiency with particular focus on excitatory neurotransmission. Tract tracing studies suggest that axonal projections are grossly normal despite the disruption of CA1 stratum pyramidale into multiple cell layers. Antibody staining for components of the excitatory circuit (e.g., glutamate receptor sub-units and transporters) did not reveal significant alterations. Intrinsic firing properties of disorganized CA1 pyramidal neurons also failed to uncover excitability defects. However, synaptic hyper-excitability was revealed in voltage-clamp

analysis of spontaneous and miniature excitatory postsynaptic currents (EPSCs) onto CA1 neurons. Significant increases in frequency were noted. This increase is consistent with enhanced glutamate-mediated excitatory drive to displaced CA1 pyramidal neurons and may contribute to cognitive and epileptic phenotypes observed.

INTRODUCTION

Lissencephaly is a central nervous system (CNS) disorder characterized by a nearly complete absence of gyri, abnormally thickened dysplastic cortex, and enlarged ventricles (Barkovich et al., 1991; Dobyns and Truwit, 1995). Mental retardation and medically intractable epilepsy are common neurological symptoms associated with this disorder. The defective gene, platelet-activating factor acetylhydrolase (PAFAH1B1, also known as *Lis1*) was identified using patient samples with hemizygous deletions of 17p13.3 (Reiner et al., 1993). Heterozygous disruption of *Lis1* in mice (homozygous deletion is embryonic lethal) results in a severe disruption of hippocampal lamination with enlarged ventricles. Studies have shown *Lis1* protein interactions with cytoplasmic dynein, its regulatory complex dynactin, and other proteins in the dynein pathway e.g., NudC, NudE, and NudEL (Morris et al., 1998; Efimov and Morris, 2000; Faulkner et al., 2000; Niethammer et al., 2000; Sasaki et al., 2000). In utero electroporation of *Lis1* small interference RNA arrests the migration of neural progenitor cells and truncates axon outgrowth (Tsai et al., 2005). *Lis1*+/- mice show impairment in the spatial learning version of a Morris water task (Paylor et al., 1999) and isolated dysplastic hippocampi are

prone to electrographic seizure-like discharge upon exposure to elevated levels of extracellular potassium (Fleck et al., 2000).

It is generally agreed that hippocampus is a critical site for the generation of abnormal electrical discharge i.e., seizures. One well-supported concept is that seizures result from over-excitation of excitatory hippocampal circuits primarily those mediated by activation of N-methyl-D-aspartate (NMDA) or alpha-amino-3-hydroxy-5-methyl-4-isoxazolepropionic acid (AMPA) type glutamate receptors (Traub and Wong, 1982; Swann et al., 1993; Lieberman and Mody, 1999; Blümcke et al., 1996; Waurin and Dudek, 2001). These observations, though most prominently supported in clinical and experimental research related to temporal lobe epilepsy, also extend to patients with focal cortical dysplasia or rodent models of malformation-associated epilepsy (Najm et al., 2000; André et al., 2004; Hagemann et al., 2003). In humans with dysplasia, expression of NMDA receptor subunits (NR2A, NR2B and NR2C) appears to be selectively increased in dysplastic neurons compared to normotopic cells (Babb et al., 1998; Ying et al., 1998; Crino et al., 2001). In the rat freeze-lesion (FL) model of polymicrogyria, NR2B subunits are functionally increased and potentially contribute to observed in vitro initiation (or propagation) of cortical seizure activity (Swann and Hablitz, 2000; Bandyopadhyay and Hablitz, 2006). In the rat methylazoxymethanol (MAM) model of nodular heterotopia, prolonged NMDA-mediated bursting and decreased GluR1 AMPA receptor subunit expression were reported (Calcagnotto and Baraban, 2005; Harrington et al., 2007). These changes in postsynaptic glutamate receptor subunit expression, if present in a *Lis1* mutant hippocampus already featuring altered dendritic arborization

(Fleck et al., 2000) and severe disorganization of the classical tri-synaptic circuit (Hirotsune et al., 1998) could have profound effects on excitatory synaptic transmission.

Although neuronal migration defects in *Lis1* mutant mice are severe and well documented, much less is known about the functional consequences of these abnormalities. A recent voltage-clamp analysis of inhibitory synaptic transmission in *Lis1*+/- mice, while showing some changes in GABA-mediated synaptic transmission and interneuron excitability, failed to identify a clearly pro-epileptic deficit (Jones and Baraban, 2007). Field recording data at the Schaffer collateral-to-CA1 excitatory synapse showed only moderate disruption of this circuit but lacked detailed analysis of excitatory synaptic transmission at the single cell level (Fleck et al., 2000). To examine circuit function in more detail, we conducted a series of anatomical and electrophysiological studies in *Lis1* heterozygote mice. Additionally, we completed an immunohistochemical analysis of GluR1, GluR2/3, NR1, NR2B, EAAC1, Glast, vGLUT1 and vGLUT2 expression. Evidence for a pro-epileptic enhancement of glutamate-mediated synaptic transmission, in the absence of gross changes in NMDA or AMPA receptor expression, is presented.

MATERIALS AND METHODS

Immunohistochemistry

A total of nine *Lis1*+/- mice (postnatal day 60) were used for immunohistochemical studies. Mice were deeply anesthetized with ketamine/xylazine and perfused via the aorta with phosphate buffered saline (PBS) followed by 4% paraformaldehyde in PBS buffer. Brains were removed and post-fixed overnight in paraformaldehyde solution, then cryoprotected in 30% sucrose PBS for 2 days. Brains were embedded in OCT medium, frozen on dry ice, and stored at -80°C. 30 μm floating sections were cut with a cryostat (Leica, Nussloch, Germany). Sections were treated with 1% hydrogen peroxide in PBS for 30 minutes, and then washed for 30 minutes in PBST (0.1% Triton X-100 in PBS). Sections were blocked in 20% goat serum in PBST for 2 hours, and then incubated with primary antibody overnight at 4°C. The following primary antibodies were used: NeuN 1:500 (Chemicon, Temecula, CA), Glial Fibrillary Acidic Protein 1:1000 (Dako), GluR1 1:250 (Chemicon), GluR2/3 1:200 (Chemicon), NR1 1:500 (Chemicon), NR2B 1:1000 (Chemicon), EAAC1/EAAT3 1:500 (Alpha Diagnostic, San Antonio, TX), Glast 1:2000 (Chemicon), VGLUT1 1:10,000 (Chemicon), and VGLUT2 1:1000 (Chemicon). After primary incubation, sections were washed for 1 hour in PBST, and then incubated in biotinylated secondary antibody (Vector Labs, Burlingame, CA; 1:500) in blocking solution for 2 hours at room temperature. Sections were then washed for 1 hour in PBST, incubated with ABC solution (Elite kit, Vector)

for 2 hours, washed for 1 hour in PBST, and developed in 0.5mg/ml diaminobenzamine (Sigma, St. Louis, MO) and 0.005% peroxide. Sections were mounted, dehydrated with alcohol and xylene washes, and coverslipped with Mount-Quick (Ted Pella, Redding, CA).

Cell counting

The tissue was prepared as described above with the following exceptions. Brains were cryoprotected in 30% sucrose PBS for 4 days. OCT embedding was done in an isopropynol alcohol, dry ice bath. The tissue was then processed, without storage, in 10 μm floating sections and stained with NeuN as described above. For each section analyzed, all NeuN positive cells were counted in a 330 μm box in CA1 (see Fig. 2). Results are expressed as total number of NeuN positive cells per 330 μm length of CA1.

Tract tracing

A total of 13 *Lis1*+/- mutants at P8 were used for the tracing experiments and 32 littermates used as control. The pups were anaesthetized and perfused transcardially with 4% paraformaldehyde in PB (pH 7.2). The brains were dissected and post-fixed in PFA for another 1–2 days at 4 °C, then were used for DiI tracing in vitro. The brains were first sectioned horizontally to expose the entorhinal cortex and hippocampus. The lipophilic dye, DiI (D3911) and DiA (D3883, Molecular Probes, Oregon, USA), were used to label

the entorhinal-hippocampal pathway and Schaffer collateral/commissural pathway, respectively. Under a dissection microscope, small crystals of the lipophilic dye were placed either in the superficial layers of entorhinal cortex (EC) or CA3. After DiI implantation, the brains were incubated in 4% paraformaldehyde in the dark at room temperature for 1-2 weeks. The brains were then sectioned horizontally using a vibratome (50 μm thickness). To visualize cell somata sections were then stained with NeuroTrace for 30 min at room temperature (1:300; Molecular probe, Eugene, OR; No. N21479). DiI labeling appears red under Rhodamine excitation whereas DiA labeling appears green under illumination of fluorescein isothiocyanate (FITC).

Image acquisition and analysis

Fluorescence images were obtained on a Zeiss LSM 510 confocal microscope (488, 594, and 633 nm wavelengths; Zeiss, Thornwood, NY). Images were prepared in Photoshop (Adobe, Mountain View, CA). Final figures were created in Adobe Illustrator software.

***In vitro* electrophysiology**

Tissue slices were prepared from male and female mice (P14-P26), as described previously (Calcagnotto and Baraban, 2005). Whole-cell voltage-clamp recordings were obtained from neurons visually identified using an IR-DIC video microscopy system.

Voltage-clamp patch electrodes (3-7 MΩ) were filled with pipette solution containing (in mM): 135 CsCl2, 10 NaCl, 2 MgCl2, 10 HEPES, 10 EGTA, 2 Na2ATP, 0.2 Na2GTP, and 1.25 QX-314 (pH 7.2; 285-290 mOsm). Current-clamp patch electrodes contained (in mM): 120 K-gluconate, 10 KCl, 1 MgCl2, 0.025 CaCl2, 0.2 EGTA, 2 Na2ATP, 0.2 Na2GTP, and 10 HEPES, adjusted to pH 7.2 with 10 M KOH (285–295 mOsm). Excitatory postsynaptic currents were recorded at 32° C from CA1 pyramidal cells in age matched *Lis1*+/- and WT littermates in normal ACSF (artificial cerebral spinal fluid) containing 5-10 μM bicuculline (to isolate excitatory currents). ACSF contained in mM: 124 NaCl, 3 KCl, 1.25 NaH2PO4, 2 MgSO4, 26 NaHCO3, 2 CaCl2, and 10 dextrose (295–305 mosM). Voltage and current were recorded with an Axopatch 1D amplifier (Axon Instruments, Foster City, CA) and monitored on an oscilloscope. Whole-cell voltage-clamp data were low-pass filtered at 1 kHz (3 dB, 8-pole Bessel filter), band-pass filtered at 60 Hz (Hum Bug, AutoMate Scientific, Berkeley, CA), digitally sampled at 2 kHz, and monitored with pClamp software (Axon Instruments, Foster City, CA). Whole-cell access resistance was carefully monitored and cells were excluded from analysis if values changed by more than 15% or exceeded 20 MΩ; only recordings with stable series resistance of less than 20 MΩ were used for analysis. Cells were held at –70 mV unless otherwise noted and the data were discarded if the holding current required to maintain this membrane potential changed by more than 15%. Data are expressed as a percentage of the baseline amplitude.

Data Analysis

sEPSCs and mEPSCs were analyzed with Mini Analysis software (Synaptosoft, Decatur, GA). An investigator blind to genotype selected events by hand. Analysis of each cell began after the cell stabilized and the drug application had washed in completely (~4 min). Decay times were measured from the time of the peak amplitude to the time at which the event was half of the peak amplitude. Histograms were constructed in Microsoft Excel from the first 50 events analyzed from each cell (WT n = 43, *Lis1*+/- n = 55). Histograms are expressed as percent of total events. Student's t-test (unpaired, nonparametric) and Kolmogorov-Smirnov test were used to determine significance. Significance was set as * = $p < 0.05$, ** = $p < 0.01$, *** = $p < 0.001$. Error bars are represented as standard error of the mean.

RESULTS/DISCUSSION

Hippocampal malformation in *Lis1* mutants

As previously reported (Hirotsune et al., 1998; Fleck et al., 2000), the hippocampus in *Lis1*+/- mice displays profound disorganization consisting of multiple CA1 pyramidal cell layers, diffusely arranged CA3 pyramidal neurons, granule cell dispersion and enlarged ventricles (Fig. 1). Immunostaining with an antibody to NeuN reveals pyramidal cell somata forming multiple distinct layers in CA1 with cells aberrantly dispersed into stratum (st.) oriens and radiatum (Fig. 1B2). Disorganized CA1 cell regions contain GFAP-positive astrocytes, but dispersed CA1 neurons are GFAP-negative as revealed in tissue sections counter-stained with cresyl violet (Fig. 1C1-2).

Disorganized regions of CA1 could contain fewer neurons if *Lis1* deficiency blocks progenitor cell neurogenesis (Tsai et al., 2005). To examine this possibility, we counted NeuN-positive cells in a 330 μm box in CA1 in thin tissue sections (see Fig. 2). We found that *Lis1* mutants and WT littermates had indistinguishable numbers of NeuN-positive CA1 cell somata (Fig. 2; WT 23 sections from 3 animals, *Lis1*+/- 32 sections from 3 animals). This suggests that despite dispersed and sometimes multiple CA1 cell layers in *Lis1* mutants, the total number of neurons is comparable to controls. *Lis1* deficiency has been proposed to block progenitor cell neurogenesis (Tsai et al., 2005). This could result in fewer newborn cells and reduced neuronal density. However, we found that the number of NeuN-positive cells in the CA1 region of hippocampus was

indistinguishable between *Lis1* mutants and WT littermates. NeuN is a neuronal specific marker, which stains not only CA1 pyramidal cells but also interneurons (Wolf et al., 1996). This raises the possibility that the ratio of glutamatergic-to-GABAergic cells changed without a change in total cell number. This is unlikely given that immunohistochemical results reported in Fleck et. al (2000) found no change in the number of interneurons using antibodies against somatostatin, parvalbumin, calbindin and calretinin. Our recent analysis of synaptic inhibition in the disorganized CA1 region of *Lis1*+/- mice also failed to detect a reduction in inhibitory postsynaptic current further arguing against a reduction in the number of GABA-expressing interneurons (Jones and Baraban, 2007).

To examine whether severe neuronal disorganization affects synaptic inputs in CA1, we performed lipophilic dye tracing in vitro (Fig. 3). A crystal of DiA (green) was placed in CA3 to label the Schaffer collateral/commissural hippocampal pathway. In WT controls, DiA-Iabeled axons terminate in st. radiatum and st. oriens in region CA1 (Fig. 3A). The gross hippocampal labeling of this pathway in *Lis1*+/- mice (Fig. 3B) was comparable to that of age-matched *Lis1*+/+ controls. A second crystal of DiI (red) was placed in layer II/III of the medial entorhinal cortex to label the perforant pathway. The perforant pathway comprises two different axonal projections in CA1 of normal hippocampus. One extends superficially along the alveus with individual fasicles running down into st. pyramidale; the other projection innervates st. lacunosum-moleculare along the hippocampal fissure (Fig. 3A). In *Lis1*+/- mice, dyslamination and disorganization of CA1 pyramidal cells did not alter these projections, and the pattern of innervations was grossly normal (Fig. 3B, B' and C). These findings suggest that axons target the correct

postsynaptic cells even when these neurons are not in their normal laminar locations. During hippocampal formation, axons are guided to their correct targets by environmental cues (Cheng et al., 2001). Abnormal lamination and aberrant distribution of principal hippocampal neurons in *Lis1* deficient mice could disrupt the development of appropriate axonal projections (Woodhams and Terashima, 2000; Drakew et al., 2002) with concomitant functional consequences (Barallobre et al., 2000; Patrylo and Willingham, 2007). Using lipophilic dyes to study axonal pathfinding (Perrin and Stoeckli, 2000), we found that the displacement of CA1 pyramidal neurons into multiple cell layers did not perturb the primary hippocampal axonal inputs to CA1 e.g., Schaffer collateral/commissural or perforant path. Although more subtle alterations such as the aberrant axonal sprouting of individual disoriented pyramidal neurons could be possible, and perhaps detectable by cell filling and camera lucida reconstruction, prior biocytin studies in *Lis1* mutant mice failed to support this possibility (Fleck et al., 2000).

Immunohistochemical studies in *Lis1* mutants

Similar to human and rodent malformations (Mathern et al., 1998; Jacobs et al., 1999; Crino et al., 2001; Harrington et al., 2007), a dysplastic hippocampus in *Lis1* mice could alter expression of postsynaptic glutamate receptor subunit(s) and/or transporter proteins required for synaptic packaging of glutamate. These possibilities were examined in a series of immunohistochemistry studies (Fig. 4). First, we used antibodies directed

against GluR1 or GluR2/3 to examine the expression of AMPA receptor subunits in *Lis1*+/- mice. In a normotopic hippocampus (*Lis1*+/+), GluR1 intensely stains the neuropil in st. radiatum, st. oriens and the dentate molecular layer. Somatic staining was also present in the pyramidal cell layer and scattered cells in the polymorphic layer of DG. This somato-dendritic distribution in control tissue is consistent with previous characterization of GluR1 in the mouse hippocampus (Rogers et al., 1991) and similar to that observed in age-matched *Lis1*+/- mice (Fig. 4A). In a normotopic hippocampus (*Lis1*+/+), GluR2/3 staining was intense in the somata of pyramidal neurons, and moderate on apical dendrites. The cellular pattern of GluR2/3 immunoreactivity in age-matched *Lis1*+/- mice was similar to WT littermates (Fig. 4B). Second, we used antibodies against NR1 and NR2B subunits to examine expression of NMDA receptors. In hippocampus of *Lis1*+/+ mice, NR1 staining was localized in apical dendrites and perisomatic membrane, where non-cellular and punctate-like staining was mostly observed. A similar staining pattern was noted in age-matched *Lis1*+/- mice (Fig. 4C). NR2B stains the soma of CA1-CA3 pyramidal cells and dentate granule cells; the dispersed principle layers were clearly detected in *Lis1*+/- mice. However, no gross alterations were found in staining intensity and cellular patterning between these animals and controls (Fig. 4D). A decrease in glutamate transporter expression could lead to a buildup of extracellular glutamate and contribute to hyperexcitability and epilepsy (Rothstein et al., 1993; Rothstein et al., 1996). To address this possibility we preformed a third series of immunohistochemical studies where we used antibodies directed against neuronal and astrocytic glutamate transporters: vGlut1, vGlut2, EACC1 and Glast. No differences were noted between the hippocampal expression patterns for these

transporters between control and age-matched *Lis1*+/- mice (Fig. 5). Taken together, these studies suggest that the primary postsynaptic receptor subunits and glutamate transport proteins required for excitatory neurotransmission are expressed in the malformed *Lis1*+/- hippocampus.

At the gross level, our immunohistochemical studies confirm prior observations on the distribution and expression patterns of GluR1, GluR2/3, NR1 and NR2B in the mouse hippocampus (Ritter et al., 2002; Hagemann et al., 2003). Although *Lis1* +/- mutants exhibit a severe disorganization and displacement of principal hippocampal neurons our immunohistochemical studies failed to uncover differences in the expression of NMDA- or AMPA-type glutamate receptor subunits. At the light microscopy level subtle changes in the dendritic distribution or trafficking of these receptor subunits could fall below the level of detection and our studies do not eliminate this possibility. Nonetheless, the key findings are that the primary components necessary for glutamatergic excitation, namely postsynaptic receptors and glutamate transporters, are present in *Lis1* +/- mutant mice and, at a gross level, are comparable to age-matched controls.

Firing properties of CA1 neurons

Input-output curves for neuronal firing frequency of neurons are a sensitive measure of ion channel expression and function. Abnormal hyper-excitable firing patterns could contribute to a pro-epileptic circuit and have been noted in a rodent model of malformation e.g., prenatal exposure to methylazoxymethanol (MAM) (Colacitti et al.,

1999; Castro et al., 2001). To address this possibility, we performed whole-cell, current-clamp recordings from visually identified CA1 pyramidal cells in *Lis1* +/- mutants and WT controls. Minor current injection was used to adjust each cell's resting membrane potential to -60 mV so that current steps could be compared across cells without normalization. Current steps were 500 ms long in 10 pA increments from 10 to 200 pA. The number of action potentials for a given current step was plotted and found to be indistinguishable between WT and *Lis1* mutant cells (Fig. 6; WT n = 8, *Lis1*+/- n = 8). There were no differences observed in firing frequency between Lis1 +/- pyramidal cells based on location in the heterotopic CA1 region. In contrast to the MAM model (Castro et al., 2001), we did not find a change in the firing frequency of dysplastic CA1 pyramidal cells arguing against an intrinsic neuronal defect and a hypothesis that membrane channel properties on dysplastic neurons are "epileptic".

Increased excitatory drive in *Lis1* +/- mutants

Enhanced glutamate-mediated excitation is a likely mechanism contributing to epileptogenesis. Indeed, two commonly used models of temporal lobe epilepsy (TLE), pilocarpine and kainic acid injection in the rat, exhibit an electrophysiologically measured increase in excitatory postsynaptic potentials or currents (Esclapez et al., 1999; Shao and Dudek, 2004). Similarly, spontaneous and miniature EPSC increases were reported in the freeze-lesion malformation model (Jacobs and Prince, 2005) and prolonged NMDA-mediated excitatory currents were reported in the MAM malformation model (Calcagnotto and Baraban, 2005). To test whether glutamate-mediated

neurotransmission is enhanced in *Lis1* +/- mutants, we recorded spontaneous and miniature EPSCs from CA1 pyramidal cells in normotopic (*Lis1*+/+) and disorganized (*Lis1*+/-) hippocampi (Figs. 7A, B and 8A, B). Under IR-DIC, pyramidal neurons were voltage-clamped at a holding potential of -70 mV in normal ACSF supplemented with a GABAA receptor antagonist (bicuculline) to isolate exciatory events. Events were blocked by subsequent addition of CNQX (20 μM) and D-APV (50 μM) to the bathing medium and reversed around 0 mV (data not shown). For isolation of miniature EPSC events bathing medium was supplemented with tetrodotoxin (1 μM TTX).

Lis1 +/- mutants showed a significant enhancement of excitatory drive with increases in the frequency of both s- and mEPSCs (Figs. 7C and 8C). To examine this change more closely, inter-event interval histograms were plotted. The cumulative fraction of EPSC inter-event intervals for *Lis1* mutants was significantly shifted to shorter intervals compared to WT controls (Figs. 7F and 8F). However, there was no change in EPSC amplitude (Figs. 7D, G and 8D, G) or decay time (Figs. 7E, H and 8E, H). These results suggest that the disorganized *Lis1* hippocampus is hyper-excitable and potentially predisposed to seizure generation.

Increased excitatory drive may be a common feature of the epileptic brain as similar findings were reported in rodent models of temporal lobe or malformation-associated epilepsy (Simmons et al., 1997; Esclapez et al., 1999; Shao and Dudek, 2004; Jacobs and Prince, 2005; Zsombok and Jacobs, 2007). In the freeze lesion model, Jacobs and Prince (2005) showed an increase in s- and mEPSCs in paramicrogyral layer V pyramidal cells. Zsombok and Jacobs (2007) confirmed these findings in the same model at a different age. An increase in sEPSCs and an increase in local connectivity have been

shown in CA1 pyramidal cells of kainate-induced epilepsy in rats (Esclapez et al., 1999; Smith and Dudek, 2002; Shao and Dudek, 2004). Esclapez and colleagues (1999) showed an increase in sEPSCs in CA1 pyramidal cells in the pilocarpine model of epilepsy in the rat. Simmons and colleagues (1997) showed an increase in sEPSCs in granule cells and mossy fiber sprouting in the same model. In another model of epilepsy, chronically injured epileptogenic sensory-motor neocortex, an increase in s- and mEPSCs was shown in layer V pyramidal cells in rats, with the change contributed to an increase in the AMPA/KA component (Li and Prince, 2002). Axonal sprouting was also shown in layer V pyramidal cells in this model (Simmons et al., 1997). In contrast to our earlier findings using rats exposed to methylazoxymethanol (MAM) in utero (Calcagnotto and Baraban, 2005) and featuring hippocampal nodular heterotopia, there was no change in the decay kinetics of EPSC events further evidence that postsynaptic glutamate receptor expression is "normal" in *Lis1* mutants.

CONCLUSIONS

Principal findings from our experiments are as follows. *Lis1* deficiency results in severe neuronal disorganization in hippocampus, as previously reported (Hirotsune et al., 1998). Hippocampal disorganization is not associated with altered axonal pathfinding or reduced numbers of CA1 pyramidal neurons. No differences in the expression of glutamate receptor subunits or associated transporter proteins were detected between WT and *Lis1* mutants. The frequency of spontaneous and miniature EPSC events was significantly increased in *Lis1* mutant mice.

An increase in spontaneous EPSC frequency could be due to an increase in (i) presynaptic neuronal activity, (ii) the number of excitatory synapses, or (iii) vesicular release (Katz, 1962). An increase in the frequency of miniature EPSCs could also be due to a proliferation of excitatory synapses and/or an increase in the probability of vesicular release as above, but not an increase in presynaptic neuronal activity since TTX is used to block action potentials in these experiments. Since we observed an increase in both s- and mEPSCs it follows that the increase in excitatory drive is most likely due to either an increase in excitatory synapses, as has been shown in other models of epilepsy (Perez et al., 1996; Smith and Dudek, 2002) or an increase in the probability of vesicular release, which has been largely unstudied in these models. Both of these possibilities fit the data and give a reasonable explanation for the hyperexcitable phenotype of *Lis1* mutants (Fleck et al., 2000).

An imbalance of excitation and inhibition is thought to underlie the pathogenesis of epilepsy (Jacobs et al., 1999; Mizielinska, 2007). Too much excitation or not enough inhibition can lead to hyperexcitability. The majority of antiepileptic drugs target the inhibitory system, with the goal of increasing GABA-mediated inhibitory drive (Löscher and Schmidt, 2006). Cortical malformations often lead to epilepsy that is unresponsive to available antiepileptic drugs (Jacobs et al., 1999; Smyth et al., 2002). Like the freeze lesion model of cortical malformation (Jacobs and Prince, 2005) our group has also found not only an increase in excitation (this Chapter) but also an increase in inhibition (Jones and Baraban, 2007). We believe that in these cases since inhibition is already enhanced trying to increase it further may not be effective but instead treatment options should be focused on decreasing excitatory drive directly. Currently there are three major drug

targets that work towards this end (reviewed in Löscher and Schmidt, 2006), (i) voltage dependant Na+ or Ca2+ channels, which would lead to a secondary inhibition of vesicular release, (ii) glutamate receptors, which would directly limit glutamatergic action and (iii) voltage-gated Ca2+ channels and vesicular release machinery, which would limit the amount of glutamate released. It is our hope that further study of this, and other models of cortical malformation, will reveal which of these targets are most effective in treating patients with intractable epilepsy.

Figure 1

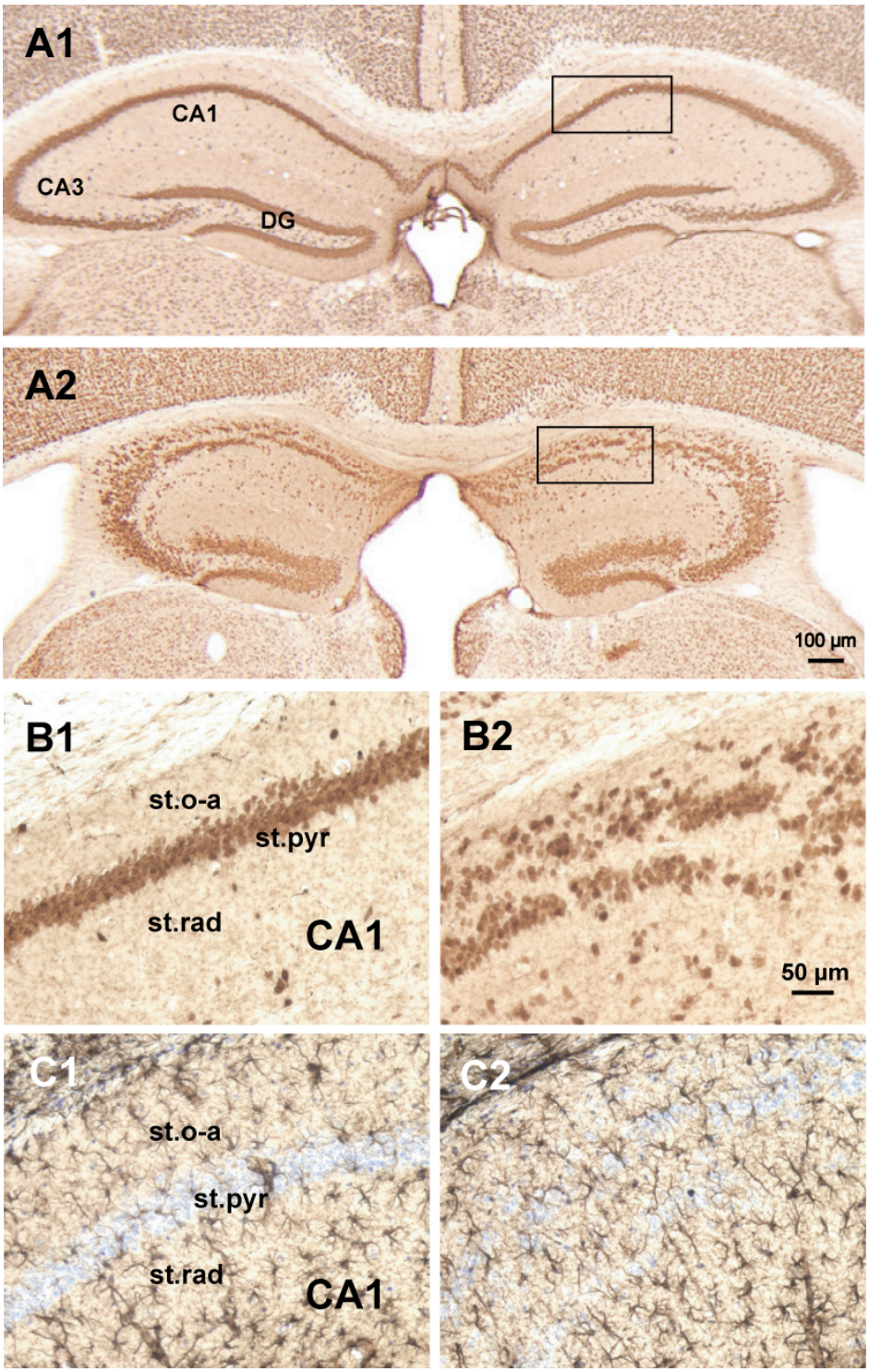
A1
CA1
CA3
DG
A2
100 µm
B1
st.o-a
st.pyr
st.rad
CA1
B2
50 µm
C1
st.o-a
st.pyr
st.rad
CA1
C2

Figure 1: Disorganization of the *Lis1*+/- hippocampus. A1: Coronal hippocampal section from a *Lis1*+/+ mouse stained with an antibody to NeuN. A2: Age-matched coronal hippocampal section from a *Lis1*+/- mouse showing severe disruption of CA1 and CA3 and enlarged ventricles. B1: Higher magnification image of CA1 (box in A1) showing the tight packing of CA1 pyramidal neurons in a normal hippocampus. B2: Same region from a *Lis1*+/- mouse showing loose packing and disorganization of the CA1 pyramidal cell region. C1: CA1 region of a *Lis1*+/+ mouse stained with an antibody to glial fibrillary acidic protein (GFAP) and counter-stained with cresyl violet. C2: Same region from a *Lis1*+/- mouse. DG: dentate gyrus; st. o-a: stratum oriens-alveus; st. pyr.: stratum pyramidale; st. rad: stratum radiatum.

Figure 2

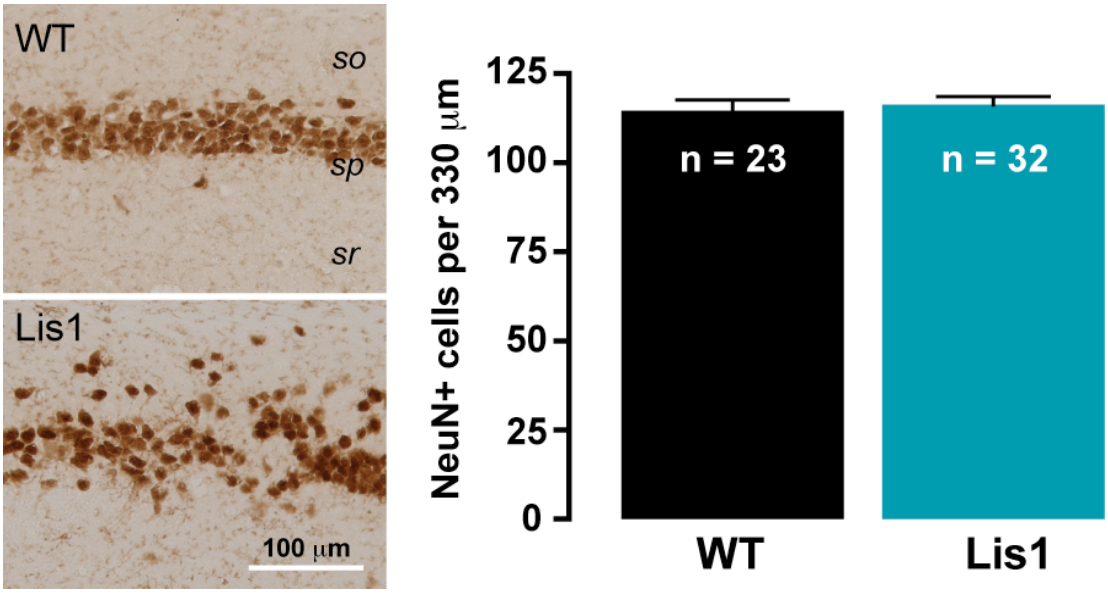
WT
so
sp
sr
Lis1
100 μm
NeuN+ cells per 330 μm
125
100
75
50
25
0
n = 23
n = 32
WT
Lis1

Figure 2: Representative 330 μm sections of CA1 stained with an antibody to NeuN. WT: wild-type *Lis1*+/+ mouse; *Lis1*: *Lis1*+/- mouse. Bar graph of all NeuN-positive cells counted in a 330 μm length of CA1 for WT (3 mice, 23 sections) and *Lis1* (3 mice, 32 sections). Data is shown as mean ± S.E.M.

Figure 3

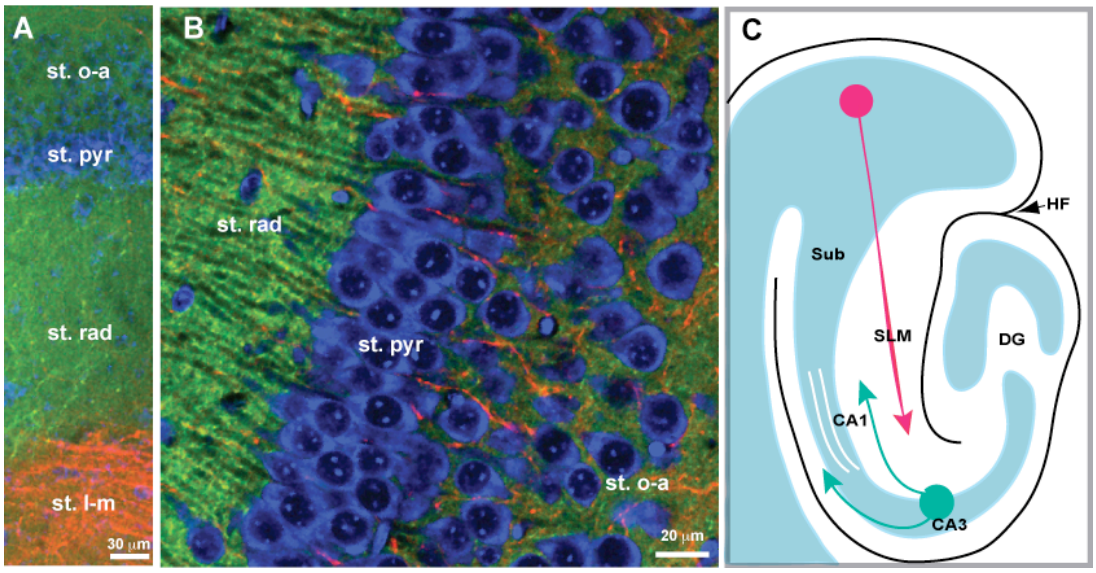
A
st. o-a
st. pyr
st. rad
st. l-m
30 μm
B
st. rad
st. pyr
st. o-a
20 μm
C
HF
Sub
SLM
DG
CA1
CA3

Figure 3: Lipophilic dye tracing in *Lis1* mutant mice. A: Section of CA1 from a *Lis1*+/+ mouse showing tightly packed CA1 pyramidal cells (blue), axonal projections from CA3 (green) and the entorhinal cortex (red). B: Same region (at higher magnification) from a *Lis1*+/- mouse showing loosely packed CA1 pyramidal neurons but otherwise normal innervation from CA3 and EC and axonal projections from EC (red) reaching throughout the disorganized CA1 cell region (blue). C: Schematic showing the principal hippocampal pathways and placement of DiI (red) and DiA (green) crystals.

Figure 4

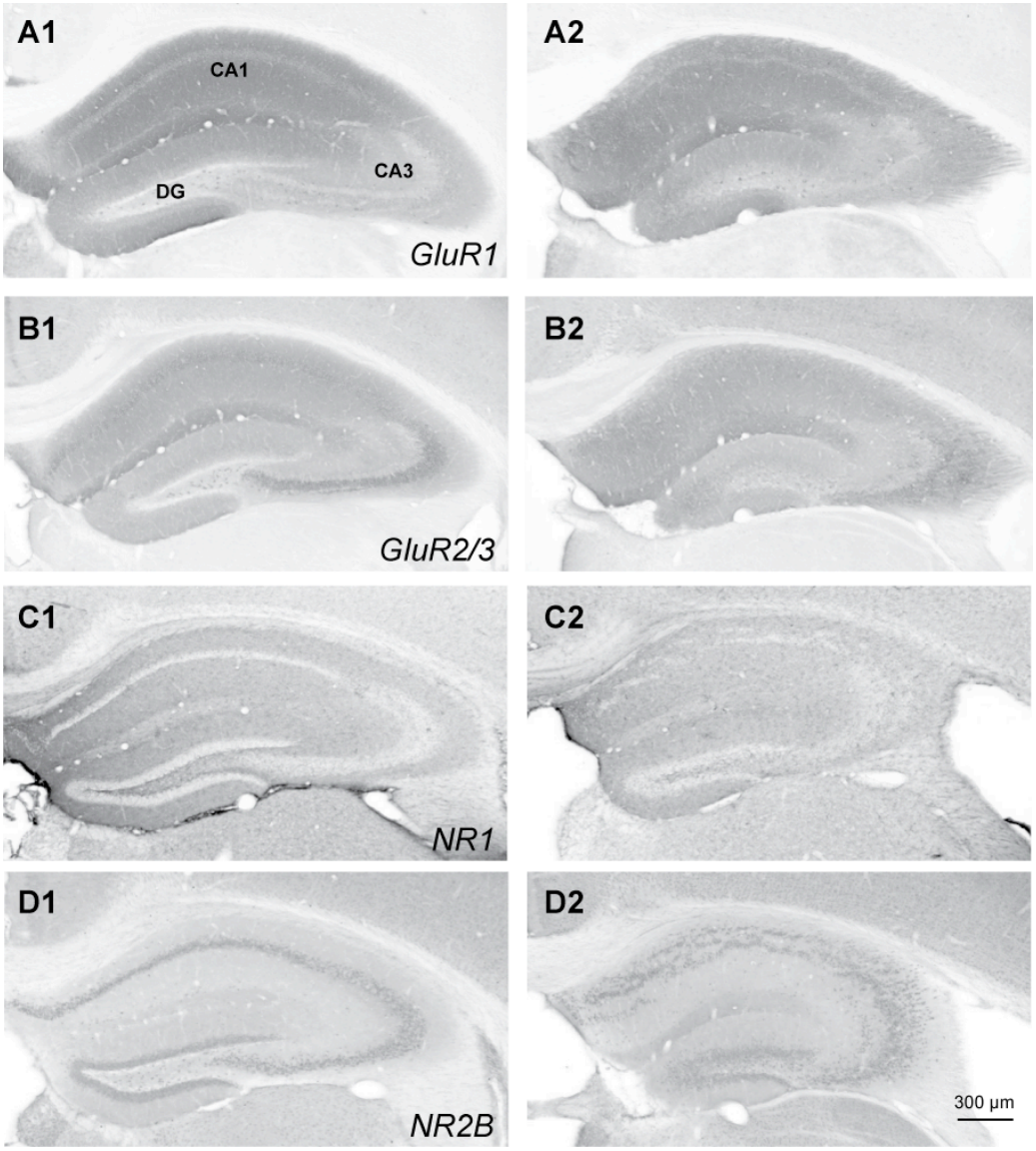

Figure 4: Glutamate receptor expression. A1: GluR1 antibody staining is shown for a representative hippocampal section from a *Lis1*+/+ mouse. A2: GluR1 staining from an age-matched *Lis1*+/- mouse. B1: GluR2/3 antibody staining is shown for a representative hippocampal section from a *Lis1*+/+ mouse. B2: GluR2/3 staining from an age-matched *Lis1*+/- mouse. C1: NR1 antibody staining is shown for a representative hippocampal section from a *Lis1*+/+ mouse. C2: NR1 staining from an age-matched *Lis1*+/- mouse. D1: NR2B antibody staining is shown for a representative hippocampal section from a *Lis1*+/+ mouse. D2: NR2B staining from an age-matched *Lis1*+/- mouse. Note: antibody staining patterns are comparable in all examples.

Figure 5

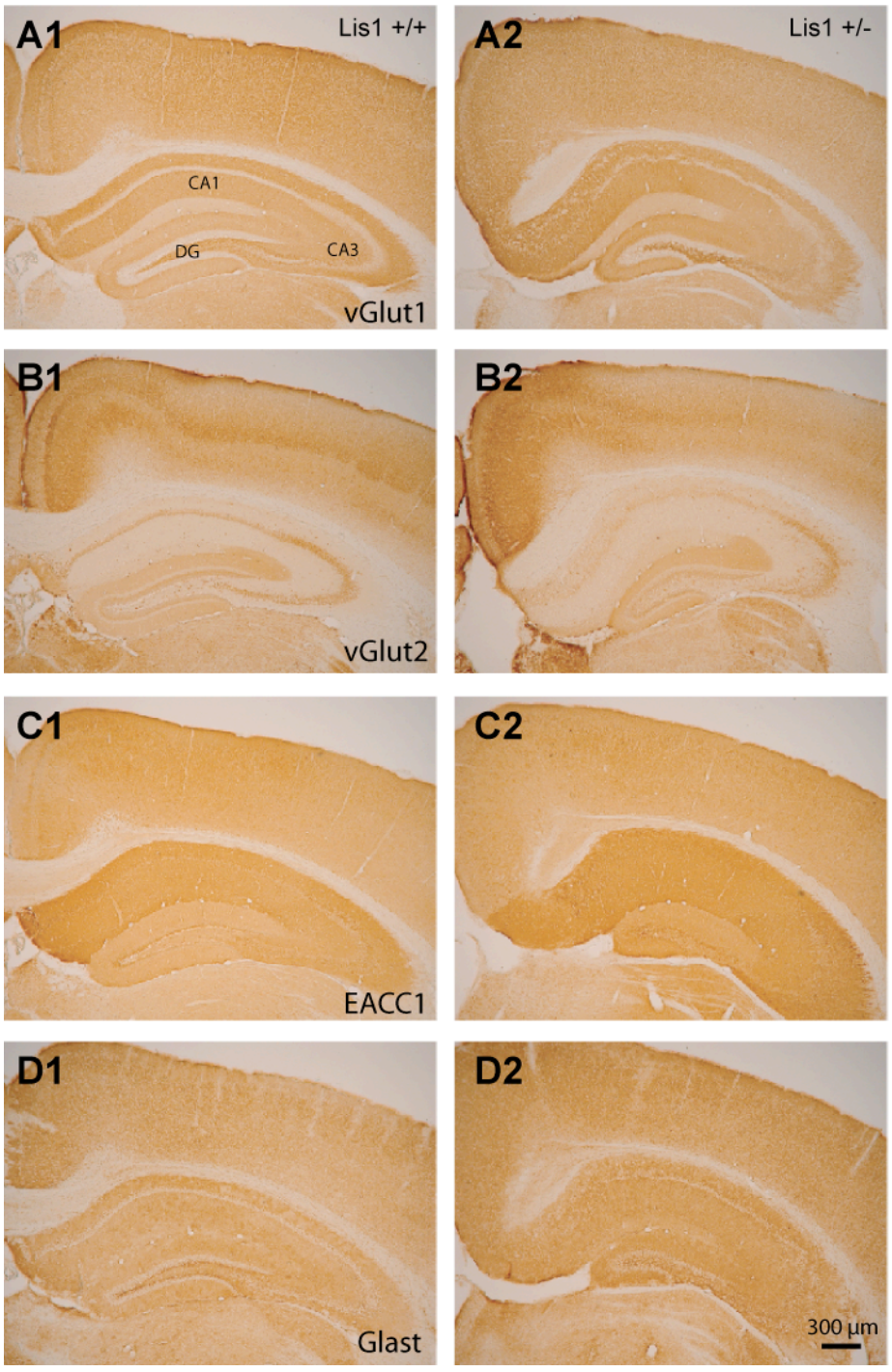
A1
Lis1 +/+
CA1
DG
CA3
vGlut1
A2
Lis1 +/-
B1
vGlut2
B2
C1
EACC1
C2
D1
Glast
D2
300 µm

Figure 5: Glutamate transporter expression in the hippocampus is comparable between *Lis1*+/+ and *Lis1*+/- mutants. Vesicular glutamate transporter one (vGlut1) heavily stained the neuropil of the hippocampus in both WT and *Lis1* mutants (A1-2). Vesicular glutamate transporter two (vGlut2) lightly stained the neuropil of the dentate gyrus and the pyramidal cell layers CA3 and CA1 (B1-2). EACC1 heavily stained the st. oriens, st. radiatum, and st. lacunosum-moleculare with weaker staining of the dentate gyrus molecular layer. EACC1 also stained the pyramidal cell layers (C1-2). Glast stained the neuropil of the hippocampus in both *Lis1*+/+ and *Lis1*+/- mutants (D1-2). Scale bar: 300 μm

Figure 6

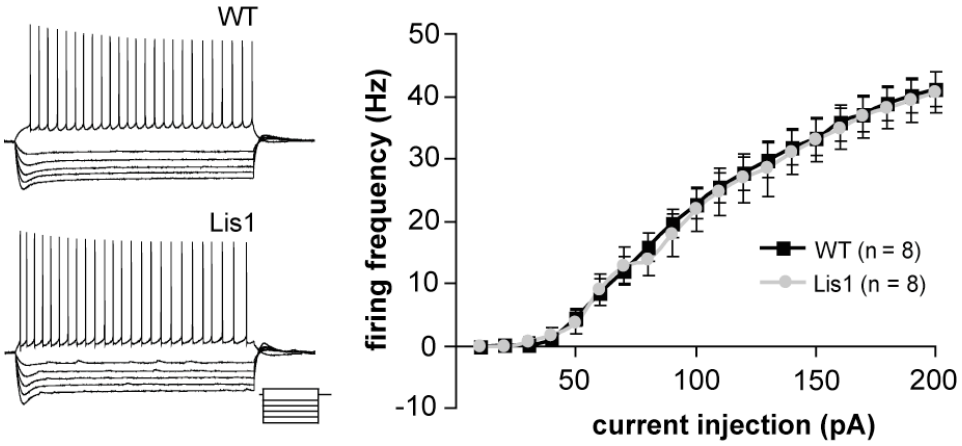
WT
Lis1
50
40
30
20
10
0
-10
firing frequency (Hz)
50
100
150
200
current injection (pA)
WT (n = 8)
Lis1 (n = 8)

Figure 6: The firing frequency of CA1 pyramidal cells is indistinguishable between WT and *Lis1* mutants. Whole cell, current clamp recordings were used to assess the intrinsic properties of CA1 pyramidal cells. Current steps were used to evoke action potentials at 10 pA intervals. Representative traces are shown from *Lis1*+/+ and *Lis1*+/- mice. The mean firing frequency and S.E.M. are plotted for each positive current step.

Figure 7

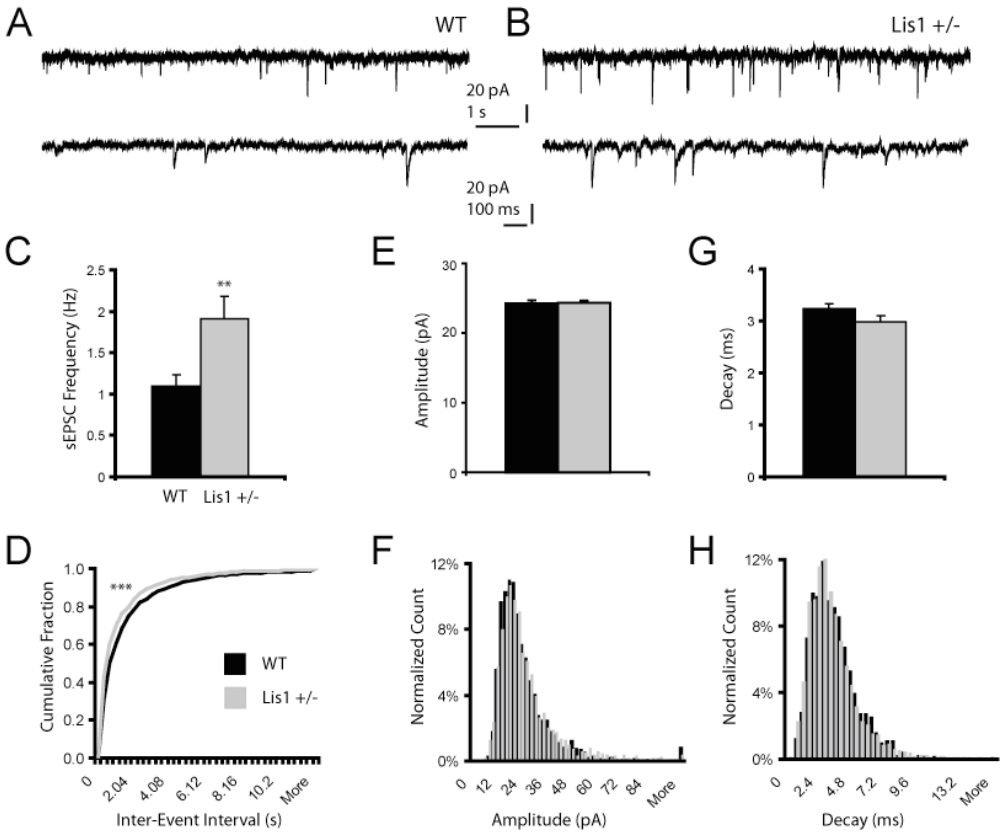
A
WT
B
Lis1 +/-
20 pA
1 s
20 pA
100 ms
C
sEPSC Frequency (Hz)
**
WT
Lis1 +/-
E
Amplitude (pA)
G
Decay (ms)
D
Cumulative Fraction
***
WT
Lis1 +/-
Inter-Event Interval (s)
F
Normalized Count
Amplitude (pA)
H
Normalized Count
Decay (ms)

Figure 7: The frequency of spontaneous excitatory postsynaptic currents (sEPSCs) is significantly increased in *Lis1* mutants. A: Sample sEPSC traces from a *Lis1*+/+ (WT) CA1 pyramidal cell. B: Sample traces from a *Lis1* mutant. Scale bars are 20 pA and 1 second for the top traces and 100 ms for the bottom traces. C: The mean sEPSC frequency is significantly increased in *Lis1* mutants [WT (black bar): 1.08 ± 0.13 Hz, n = 43; *Lis1*+/- (gray bar): 1.95 ± 0.27 Hz, n = 55; Students t-test $p \leq 0.005$]. D: Bar plot of sEPSC amplitude. E: Bar plot of sEPCS decay time (measured between the peak amplitude and the half amplitude). F: The cumulative fraction of inter-event intervals of sEPSCs was significantly different in *Lis1* mutants, with a shift towards shorter inter-event intervals (WT: 2084 events; *Lis1*+/-: 2666 events; KS test $p < 0.0001$). G: The distribution of sEPSC amplitudes was similar between WT (black) and *Lis1* mutants (gray). Data is shown as mean ± S.E.M. for all bar graphs (C-E). The nonparametric, students t-test was used to compare frequency and the Kolmogorov-Smirnov (KS) test was used to compare the cumulative inter-event intervals in F. ** $p< 0.01$, *** $p < 0.001$

Figure 8

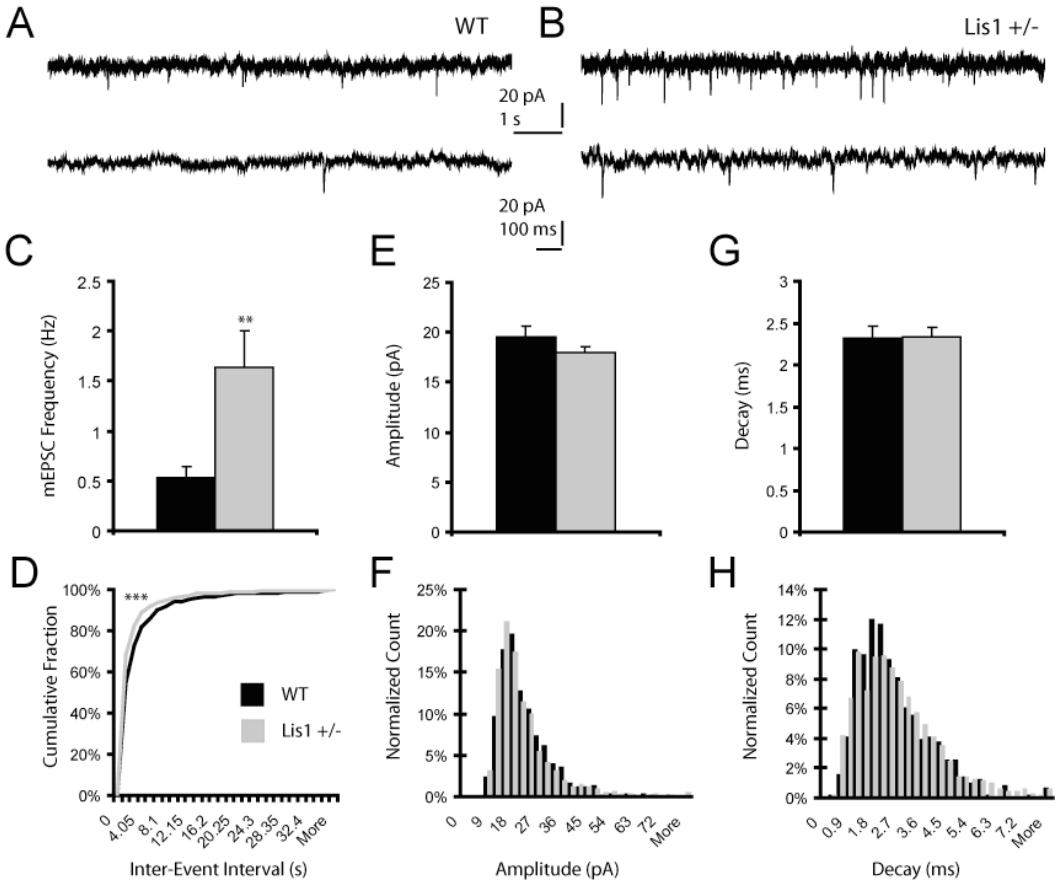
A
WT
B
Lis1 +/-
20 pA
1 s
20 pA
100 ms
C
mEPSC Frequency (Hz)
**
E
Amplitude (pA)
G
Decay (ms)
D
Cumulative Fraction
***
WT
Lis1 +/-
Inter-Event Interval (s)
F
Normalized Count
Amplitude (pA)
H
Normalized Count
Decay (ms)

Figure 8: The frequency of miniature excitatory postsynaptic currents (mEPSCs) is significantly increased in *Lis1* mutants. A: Sample mEPSC traces from a wild-type (WT) CA1 pyramidal cell. B: Sample traces from a *Lis1* +/- mutant CA1 pyramidal cell. Scale bars are 20 pA and 1 second for the top traces and 100 ms for the bottom traces. C: The mean mEPSC frequency is significantly increased [WT (black bar): 0.54 ± 0.10, n = 16, *Lis1*+/- (gray bar): 1.64 ± 0.36, n=45; Students t-test $p \leq 0.005$]. D: Bar plot of mEPSC amplitude. E: Bar plot of mEPSC decay time constant. F: The cumulative fraction of inter-event intervals is significantly shifted towards shorter times (WT: 619 events, *Lis1*+/-: 1944 events, KS test $p < 0.0001$). G: The distribution of mEPSC amplitude is normal. H: The distribution of the decay times is normal. WT: 635 events; *Lis1*+/-: 1989 events for amplitude and decay measurements. Data is shown as mean ± S.E.M. for all bar graphs (C-E). The nonparametric, students t-test was used to compare frequency and the Kolmogorov-Smirnov (KS) test was used to compare the cumulative inter-event intervals in F. ** $p< 0.01$, *** $p < 0.001$

CHAPTER TWO

Heterozygous *Lis1* Mutation Leads to Increased Glutamatergic Vesicle Pool Size and Seizures in Mice

ABSTRACT

Lis1 was the first protein identified in Type I lissencephaly, a human neuronal migration disorder, characterized by mental retardation, shortened lifespan, and epilepsy. *Lis1* has been extensively studied for its role in neuronal migration, its interaction with the dynein/dynactin complex, its influence on microtubule directed transport, and its role in epilepsy. *Lis1* +/- mice have severely disrupted neuronal organization, especially in the hippocampal formation, owing to the role of *Lis1* in neuronal migration. However, why humans with lissencephaly or why *Lis1* +/- mutant mice have seizures has never been elucidated. We show, for the first time, a potential mechanism for hyperexcitability and seizures in *Lis1* haploinsufficient mice. Surprisingly, hyperexcitability may not be directly related to problems associated with aberrant neuronal migration as has been long supposed, but rather due to a role of *Lis1* in glutamatergic, vesicular transport. In mutant

mice, a deficit in *Lis1* protein leads to accumulation of glutamatergic, synaptic vesicles demonstrated here using electron microscopy and voltage-clamp recordings. This increase in vesicle number is associated with increased glutamate release, changes in short-term potentiation and ultimately seizures. These results not only change the way we think about brain malformations and lissencephaly, they point towards an alternative approach to treating this disease.

INTRODUCTION

Lissencephaly is a brain malformation disease, characterized by mental retardation, shortened lifespan, and epilepsy (Barkovich et al., 1991; Dobyns and Truwit, 1995). *Lis1* was the first protein discovered in Type I lissencephaly and is also called PAFAH1B1 (the β subunit of platelet-activating factor acetylhydrolase) (Reiner et al., 1993). Lissencephaly is a haploinsufficiency disease meaning that only one copy of the gene needs to be mutated (Dobyns and Truwit, 1995). To study this devastating disease, Hirotsune and colleagues developed a mouse model with one inactive copy of *Lis1*. As with humans, homozygous *Lis1* mice are embryonic lethal (Hirotsune et al., 1998), so in this study *Lis1* +/- (heterozygous) mutants are used. The cortical malformations in human lissencephaly patients and the *Lis1* +/- mutant mouse are dramatic so it is no surprise that the majority of work done on *Lis1* has been focused on understanding its role in neuronal migration. This work has shown that *Lis1* interacts with the dynein/dynactin complex and is critical for microtubule dynamics, kineticore orientation, and translocation of the nucleus during neuronal migration (most recently reviewed by:

Kerjan and Gleeson, 2007; Wynshaw-Boris, 2007; Kawauchi and Hoshino, 2008). The *Lis1* protein has also been show to interact with the dynein/dynactin complex. Some work has been done on the mouse mutant looking at the function of the brain post migration (Fleck et al., 2000; Jones and Baraban, 2007, also see Chapter One). Fleck and colleagues (2000) found an increase in hyperexcitability in hippocampal slices from lis1 +/- mutants in raised extracellular potassium (K+). Our lab recently published a study on interneuron function in the hippocampus of Lis1 +/- mutants, which found that inhibitory function was intact, although somewhat elevated in drive (Jones and Baraban, 2007). In Chapter One, I present work done in the excitatory system where I find that the glutamatergic system is relatively normal; however, the excitatory drive and spontaneous glutamatergic events are nearly doubled. Despite over a decade of research on *Lis1* and the *Lis1* +/- mouse, no clear mechanism of seizure generation has been elucidated.

In this study, we present electroencephalographic (EEG) evidence for spontaneous seizure activity, an enlarged glutamatergic Shaffer collateral/CA1 (SC/CA1) readily releasable (RRP) and total vesicular pool, enhanced short-term plasticity, and *in vitro* rescue with reduced calcium (Ca^{2+}) entry. These results demonstrate a clear presynaptic defect in the excitatory system, which may underly the enhanced excitability and ultimately seizures in *Lis1* +/- mice.

METHODS

Electroencephalography

Six *Lis1* +/- mutants and 4 WT littermates (P36-P49) were recorded for 7-7.5 hours a day for up to 5 non-consecutive days (generally alternating recording days up to 10 days). 35-40 hours of recording were done per animal. Surface, head mount EEG hardware was purchased from Pinnacle Technology, Inc. (Lawrence, KS). Mice were anesthetized and the surface of the skull was exposed with a single rostral/caudal incision. Head mounts were attached with four conductive screws, which also acted as the electrodes for the recording. Two wires were laid on top of the shoulder muscles, under the skin, for EMG recording. Dental cement was used to secure the mount and mice were allowed to recover for four days before recording. A swivel mount on the attached wires allowed the mice to freely move about the recording chamber. There was hardware preamp gain of 10 times and a main hardware amplifier gain of 50.78 times. Recordings were sampled at 400 Hz and high pass filtered at 1 Hz for the EEG and 10 Hz for the EMG. Low pass filtering was done at 40 Hz (EEG) and 100 Hz (EMG). Video was taken during recordings for later confirmation of seizure activity.

Electron Microscopy

Animlas were processed using standard procedures (Kuo, 2007). Briefly, three *Lis1* +/- mutants and two WT littermates were perfused and fixed with 2% paraformaldehyde and

2% glutaraldehyde for 5 hours. Samples were then cut into 50 μM sections on a vibratome. They were then osmicated, dehydrated in a series of alcohol washes, and embedded in Epon Resin. The Shaffer collateral/CA1 synapse region was isolated, ultrathin sections were cut (80 nm) and stained with Uranyl acetate (1%, 10 minutes) and lead citrate (10 minutes). Sections were observed and photographed (at 14,000 times magnification) with a JEOL 100c microscope.

Ultrastructural analysis

Sections were taken from the striatum radium in the CA1 region of the hippocampus. Synapses were selected for study if the presynaptic terminal was intact and the synaptic cleft and postsynaptic density were discernable as asymmetric. An investigator blind to the genotype of the animals used NIH software (Image J) to measure the area of the presynaptic terminal, the length of the postsynaptic density (PSD), and the distance from the center of each vesicle to the closest point on the PSD. Vesicles were considered docked, for this study, if they were within 50 nm or less from the closest point on the PSD.

***In Vitro* Electrophysiology**

Tissue slices were prepared from male and female mice as described previously (Calcagnotto and Baraban, 2005). Whole-cell voltage-clamp recordings were obtained from CA1 pyramidal cells visually identified with IR-DIC video microscopy. Voltage-

clamp patch electrodes (3-7 MΩ) were filled with pipette solution containing (in mM): 135 CsCl2, 10 NaCl, 2 MgCl2, 10 HEPES, 10 EGTA, 2 Na2ATP, 0.2 Na2GTP, and 1.25 QX-314 (pH 7.2; 285-290 mOsm). Recordings were made in nACSF containing (in mM): 124 NaCl, 3 KCl, 1.25 NaH2PO4, 2 MgO4, 26 NaHCO3, 2 CaCl2, and 10 dextrose (295–305 mOsm). All whole-cell recordings were obtained in nACSF and then the bathing medium was switched to nACSF with 5-10 μM bicuculline to isolate glutamatergic currents. Experimental manipulations were started after bicuculline had fully washed in and the recording had stabilized, typically four to five minutes after break in. Cadmium (Cd^{2+}) was added to the bathing medium in experiments indicated, by diluting a stock of $CdCl_2$ solution into the bathing media. For all experiments with evoked responses, a bipolar stimulation electrode was placed near CA3 in the Shaffer collateral fiber bundle.

RESULTS/DISCUSSION

Spontaneous EEG seizure activity in Lis1 +/- mutants

Hyperexcitability of hippocampal slices from *Lis1* +/- mutants has been shown previously (Fleck et al., 2000, and Chapter One); however, *in vivo* seizures have not been documented in these animals. Hirotsune and colleagues (1998) reported one, observed, lethal seizure in the *Lis1* +/- mutant. They then speculated that the 3-5% of mutant mice that died in the 3-5 week age range might have died of seizures. While some authors take that speculation as fact (Reiner et al., 2002; Valdés-Sánchez et al., 2007), no data has

ever been published demonstrating seizure activity in a *Lis1* +/- mutant. Here we provide, for the first time, evidence for spontaneous electrographic seizures in the *Lis1* +/- mutant (Figure 1). Cortical spikes (Figure 1B, arrowheads) were seen in all (6/6 animals) of the *Lis1* +/- mutants recorded and were not observed in WT controls (4 animals). Spontaneous electrographic seizure activity, defined as the presence of polyspikes (or sharp high-amplitude spiking) lasting over 10 seconds in duration was seen in 33% (2/6) *Lis1* +/- mutants in the period of observation (Figure 1C) and never seen in WT controls (4 animals). Representative examples of EEG activity are shown in Figure 1.

Electron Microscopy and Ultrastructural analysis:

Lis1 Haploinsufficiency Leads to an Enlarged Glutamatergic Vesicle Pool

In our recent study of Lis1 +/- mutants, we found an increase in miniature excitatory postsynaptic currents (mEPSCs) recorded in CA1 pyramidal cells (Chapter One). mEPSC frequency has been shown to be dependent on vesicular release probability (p) and the number of release sites (n) (reviewed in Fisher et al., 1997; Zucker and Regehr, 2002). There are several ways to increase n. Unmasking of previously silent synapses (Isaac et al., 1995), creation of new synapses or synaptic contacts (Wojtowicz et al., 1994), or increasing the number of vesicles in the readily releasable pool (RRP) (Smith, 1999; Toonen et al., 2006). Lis1 has been shown to interact with the dynein/dynactin complex and regulate retrograde, microtubule directed transport (Sasaki et al., 2000). Two lines of evidence show that glutamatergic vesicles are transported, retrogradely,

away from the synapse: (i) in axon crush experiments, glutamatergic vesicles accumulated at the injury site (Li et al., 2000) and (ii) in a study where P-150 glued, a crucial component of the dynactin complex, was engineered with a point mutation that disrupts its function in the dynactin complex (and thus disrupts retrograde transport) vesicles were seen to accumulate at the neuromuscular junction (NMJ) (Lai et al., 2007). As such, an intriguing possibility of the consequences of heterozygous Lis1 mutation is that disrupting Lis1 function could lead to accumulation of synaptic, glutamatergic vesicles explaining the increase in mEPSCs seen in this mutant.

To examine this possibility, we performed an electron micrograph (EM) ultrastructural analysis of CA1 glutamatergic (asymmetric) synapses (Figure 2). Although levels of *Lis1* protein have been shown to affect microtubule stability (Sapir et al., 1997) and changes in microtubule stability could lead to structural changes of the synaptic terminals we found that the terminal area of *Lis1* +/- mutants was similar to WT controls (Figure 2C, WT 0.24 ± 0.02 μm^2; *Lis1* +/- 0.27 ± 0.02 μm^2). Another structural explanation for the previously observed increase in mEPSCs (Chapter One) in the *Lis1* +/- mutant is an increase in either the total postsynaptic density (PSD) length or an increase in the number of synaptic contacts per terminal. We next examined both of these possibilities and found that the mean PSD length, and the total PSD length per terminal were comparable between *Lis1* +/- mutants and WT animals (Figure 2D, WT 210 ± 11 nm; *Lis1*+/- 224 ± 8 nm). These results indicate that the basic structure of the synapse is intact in the *Lis1* +/- mutant animals and there is not a proliferation of synaptic contacts, per terminal, in the *Lis1* +/- mutant (Figure 2C and 2D). Because reduced retrograde transport could lead to the accumulation of synaptic vesicles (Lai et al., 2007),

we next counted the total number of synaptic vesicles for each synaptic cross section and found that the mean number of synaptic vesicles in *Lis1* +/- mutants was significantly higher than WT controls (Figure 2E, WT 33 ± 3; *Lis1* +/- 53 ± 3; $p \leq 0.001$). The total number of synaptic vesicles is not necessarily related to the number of vesicles in the readily releasable pool (Rizzoli and Betz, 2005) so we went on to examine the distribution of synaptic vesicles relative to the PSD. Image J (NIH) was used to record the location of each vesicle and custom python scripts were written to calculate the distance between each vesicle and the closest point on the PSD. Vesicles within 50 nm of the PSD were considered docked for this study (Kushner et al., 2005). We found that the RRP was significantly larger in *Lis1* +/- mutants than WT controls (Figure 2F, WT 2.3 ± 0.2; *Lis1* +/- 4.9 ± 0.3; $p \leq 0.001$). This increase in the RRP explains the increase in mEPSC frequency similar to other studies that have also seen an increase in the RRP (Tyler and Pozzo-Miller, 2001; Kushner et al., 2005; Virmani et al., 2005; Toonen et al., 2006).

Lis1 +/- Mutants have Enhanced Facilitation and a Functioning Recycling Pool of Vesicles

The recycling pool of vesicles replenishes the RRP and is critical for maintaining synaptic transmission under repetitive stimulation (reviewed in Rizzoli and Betz, 2005). Because of *Lis1*'s effect on vesicular trafficking it is possible that vesicles in the reserve pool are unable to be moved into the RRP and thus the *Lis1* +/-mutant synapse would experience synaptic depression as seen in the Rab3a mutant (Geppert et al., 1994). It is

also possible that since the total vesicle pool is enlarged in the *Lis1* +/- mutant (Figure 2E, 2F), unlike the Rab3a mutant, that the recycling pool of vesicles is functioning properly. To test these two different possibilities, we used a repetitive stimulation protocol (10Hz for 3 seconds of the SC-CA1 synapse) and single-cell voltage-clamp recordings from visually identified dysplastic CA1 pyramidal neurons. This protocol combined with pharmacological isolation of postsynaptic glutamate-receptor mediated synaptic events allowed us to examine the recycling pool of vesicles in the *Lis1* +/- mutant (Figure 3). We found that the *Lis1* +/- mutant was able to sustain high levels of synaptic transmission under repetitive stimulation. This indicates that the vesicular trafficking mechanisms responsible for moving recycling vesicles into the RRP are intact and functioning. As previously discussed, it appears that *Lis1* has an important role in retrograde transport; however, this does not appear to affect the mechanisms responsible for moving the recycling vesicles into the RRP (Toonen et al., 2006 and reviewed in Rizzoli and Betz, 2005; Santos et al., 2008). An intriguing observation from this experiment was an elevation of the facilitation of the response in *Lis1* +/- mutants compared to WT controls. Specifically, it appears that the paired pulse facilitation (PPF), measured as the second pulse divided by the first pulse (see the first two EPSCs in the train in Figure 3A, 3B) was greater in *Lis1* +/- mutants. Because enhanced facilitation could underlie enhanced excitability in these mice we next examined short-term plasticity in these animals.

Enhanced Short-Term Facilitation in Lis1 +/- mutants

Paired Pulse facilitation (PPF) is a sensitive measure of presynaptic vesicular release. PPF has been shown to be of presynaptic origin in all systems studied and to be an increase in quanta (n) released for an action potential (AP) without a change in the postsynaptic response properties or a change in quantal size (reviewed in both Fisher et al., 1997; Zucker and Regehr, 2002). Calcium entry into the presynaptic terminal is required for the release of neurotransmitter filled vesicles and the amount of vesicular release is directly related to the level of presynaptic calcium entry (Atwood, 1976; Kreitzer and Regehr, 2000; Zucker and Regehr, 2002). There are several controlling factors to consider for changes in PPF. PPF is thought to be due to residual Ca^{2+} in the presynaptic terminal from the first pulse. However, synaptic depression is also active at the same time. Synaptic depression is generally thought to be due to a depletion of the readily releasable pool (RRP) of synaptic vesicles and dominates facilitation at many synapses (Zucker and Regehr, 2002). This appears to be the case in WT Shaffer collateral-CA1 synapses. Classic studies at this synapse have shown that the paired pulse ratio (second pulse divided by the first pulse) is inversely proportional to the probability of release (Manabe et al., 1993; Asztely et al., 1996). In these studies the probability of release was altered by either increasing the concentration of extracellular Ca^{2+} (increasing the probability of release) or adding agents in the bathing media that decreased Ca^{2+} entry (such as CdCl2, a competitive inhibitor of presynaptic Ca^{2+} entry) and thus the probability of release[1] (Manabe et al., 1993; Asztely et al., 1996). These manipulations had a larger effect on the first pulse than the second pulse. This is evident in Figure 1 of

[1] The aim of these studies was to demonstrate that long-term potentiation was postsynaptic in origin. They did this by monitoring PPF before and after LTP induction. They were able to show that since PPF did not change with LTP then LTP must be postsynaptic in origin.

Manabe (1993) where the authors measure PPF in 2.5 mM Ca^{2+}[external] and then again after raising the external Ca^{2+} concentration to 4 mM. The second pulse is nearly identical at both concentrations of external calcium where the first pulse doubles in size when the external calcium is elevated. Since a near maximal response for the second pulse was achieved in 2.5 mM Ca^{2+}[external] then increasing the Ca^{2+} entry by elevating the external concentration would only be expected to increase the response to the first pulse. Indeed, this experiment clearly demonstrated that the second pulse is saturated under these conditions and thus increasing the probability of release in this system is expected to decrease PPF (second pulse/first pulse). Another often-cited study, Asztely F. (1996), that showed this relationship, reported experiments in which all slices were bathed in a high concentration of external Ca^{2+} (4mM). As such, these studies focused on a saturated synapse and effects of synaptic depression (depletion of the RRP). When the second pulse is at or near saturation then these manipulations affect the first (smaller) pulse to a greater extent. The *Lis1* +/- mutant, however, has a larger RRP and thus is expected to not saturate as quickly, especially with a more physiological external Ca^{2+} concentration of 2 mM. This means that the *Lis1* +/- mutant may have greater PPF than WT animals. We measured PPF with the near physiological external concentration of Ca^{2+}, 2mM, and found that the *Lis1* +/- mutants had elevated PPF (figure 3A, 3B). Whole cell recordings were obtained from visually identified CA1 pyramidal cells in *Lis1* +/- mutants and WT littermates. Shaffer collateral stimulation (50 ms ISI) was used to elicit an evoked response between 50 and 100 μA. Occasionally stimulation had to be reduced (to achieve an initial response of slightly less than 50 μA when the second response was exceptionally large), see Figure 4C(iii). Lis1 +/- mutants had a

significantly higher PPR (Figure 4A, 4B; 3.0 ± 0.3; 6 animals, 29 cells) than WT littermates (1.4 ± 0.06; 8 animals, 31 cells). Significance was measured using a two tailed, unpaired t-test ($p < 0.0001$). This result is corroborated by a study done in a mouse where the RRP is larger than WT animals and an increase in the RRP lead to an increase in PPF (Kushner et al., 2005).

Reduced Calcium Entry Rescues PPF in Lis1 +/- Mutants

As discussed above, investigators have found, at WT SC/CA1 synapses, an inverse relationship between PPF and the probability of release (Manabe et al., 1993; Asztely et al., 1996; Wang et al., 2008). It is clear that synaptic depression (or the size of the RRP) is critical in these experiments (discussed in (Zucker and Regehr, 2002). Because the RRP is limiting at the WT SC/CA1 synapse it is not surprising that the opposite manipulation, decreasing Ca^{2+} entry, should increase the PPF in this synapse under these conditions. Indeed, in WT animals, adding high concentrations (60-100 uM) of CdCl2 to the bathing media were shown to increase the PPF in the Shaffer collateral-CA1 synapse (Wang et al., 2008). In a recent study by Shu Wang and colleagues (2008), they show in Figure 2A that application of 60 uM Cd^{2+} to the bath reduces the first EPSC by 50% and the second by only 25%. If the second pulse is already near saturation under basal conditions then reducing the probability of release is expected to affect the first pulse by a greater degree than the second pulse – hence, the inverse correlation of probability of release to PPF. It is easy to imagine this relationship for any synapse where the second pulse is at or near saturation. However, this is not always the case. In

other synapses and even in the SC-CA1 synapse, in a mutant animal, the opposite has been reported (Dudel, 1990; Zengel et al., 1993a; Zengel et al., 1993b; Doussau et al., 1998; Kushner et al., 2005), and reviewed in (Zucker and Regehr, 2002). Because the facilitation of the second pulse is thought to be a result of residual calcium from the first pulse, in a synapse that is not near saturation, one would expect the second pulse to be as, if not more, sensitive to changes in presynaptic calcium entry. Several studies have showed that when calcium entry has been limited in synapses that are not saturated or under synaptic depression, PPF decreases (Dudel, 1990; Zengel et al., 1993a; Zengel et al., 1993b; Doussau et al., 1998 and reviewed in Zucker and Regehr, 2002). Zengel and colleagues (1993a) showed that application of omega-Conotoxin (an inhibitor of presynaptic calcium channels) to the neuromuscular junction (NMJ) had a larger reducing affect on the second pulse than the first and thus caused a reduction of PPF (Zengel et al., 1993b - figure 1B). Importantly, raising the extracellular concentration of Ca^{2+}, showing that the effect was directly related to calcium entry, reversed this effect. Later that year, the same group added other Ca^{2+} channel blockers, including Cd^{2+}, and observed the same effect (Zengel et al., 1993a) e.g., reducing presynaptic calcium entry reduced the PPR. An interesting study that looked at the effect of hyperphosphorylation of synapsin I by expression of a constitutively active form of H-ras (Kushner et al., 2005) found that the RRP of SC-CA1 synapses was enlarged in these animals. They also observed an increase in mEPSC events in autaptic neurons and an increase in mEPPs (miniature end plate potentials) at the NMJ – similar to what we found in hippocampal slice from *Lis1* +/- mutant (Chapter One, Figure 8). These results show that the probability of release is enhanced in these mutants. If the synapse were near saturation, then one would expect

the animal to have less PPF; however, if the synapse is not saturated then an increase the PPF is possible. Kushner and colleagues (2005) reported an increase in PPF at the SC-CA1 synapse. This result makes sense when one considers that an increase in the RRP could change the dynamic range of the synapse and mean that it is, in fact, further from saturation than a WT synapse under the same conditions (as discussed above).

Another final consideration is that homeostatic plasticity may be in play under these conditions. It is well established that synaptic activity can be modulated in response to neuronal activity levels (reviewed in Burrone and Murthy, 2003; Turrigiano and Nelson, 2004). It is reasonable to expect that a mutation that leads to an enlarged RRP, and spontaneous release, would also be under homeostatic control. This means that under basal conditions, even with an enlarged RRP, single evoked responses could be relatively normal. However, when the system is pushed, such as with paired or trains of pulses, these compensatory mechanisms could be overwhelmed. In the *Lis1* +/- mutant, like the H-ras mutant (Kushner et al., 2005) mouse above, we noted an enlarged RRP (figure 2F). Similar to that study, we also observed an increase in PPF compared to WT littermates (Figure 4A). Since we observed an increase in PPF it would appear that the *Lis1* +/- mutant SC-CA1 synapse is not saturated or near saturation. If this is true, we should see a decrease in the PPR when presynaptic calcium entry is decreased similar to studies done in synapses or conditions where the synapse is not saturated (Dudel, 1990; Zengel et al., 1993a; Zengel et al., 1993b; Doussau et al., 1998 and reviewed in Zucker and Regehr, 2002). When a low level of extracellular Cd^{2+} (20uM) was introduced into the bath, PPF was reduced to WT levels in all cells tested (figure 4C-4E, Lis1 +/- 0 μM Cd2+,3.0 ± 0.5; Lis1 +/- 20 μM Cd2+, 1.5 ± 0.1; 2 animals, 11 paired (both conditions)

cells compared to WT, 1.4 ± 0.06; 8 animals, 31 cells). This further supports the theory that the *Lis1* +/- mutant SC-CA1 synapse, which has an enlarged RRP, is not saturated or near saturation as has been seen for this synapse in WT animals in other studies (Manabe et al., 1993; Asztely et al., 1996; Wang et al., 2008). Because the *Lis1* +/- mutant, PPF phenotype was rescued by limiting Ca^{2+} entry, it follows that this is a potential mechanism for treatment of lissencephaly.

CONCLUSIONS

The brain malformations of lissencephaly patients and the *Lis1* +/- mutant mouse are severe and so it is no surprise that the majority of research on this gene have focused on how *Lis1* is involved in neuronal migration. It has generally been assumed that the role *Lis1* plays in seizure generation is during development, with the formation of the disorganized brain. We have previously showed (Chapter One) that despite a failure to form a normally laminated hippocampus, excitatory transmission in these mice is largely normal, although elevated. Here we have show that the *Lis1* protein has a previously unappreciated role in glutamatergic transmission.

An enlarged vesicular pool, especially the RRP, explains several key aspects of seizure generation in *Lis1* +/- mutants. Elevated glutamatergic transmission in the hippocampus appears to be largely due to spontaneous release of glutamatergic vesicles (see Chapter One). An increase in spontaneous release events has also been seen in other models where the RRP is enlarged (Tyler and Pozzo-Miller, 2001; Kushner et al., 2005; Virmani et al., 2005; Toonen et al., 2006; Srinivasan et al., 2008). We also show

changes in short-term plasticity, which could directly contribute to hyperexcitability and ultimately seizure generation. There are two potential reasons the observed increase in PPF in Lis1 +/- mutants. An enlarged RRP means that the mutant synapse is no longer saturated with small increases in internal Ca^{2+} concentration (residual Ca^{2+} from the first or first several pulses). The second mechanism that may be in play is some form of homeostatic control, which is reducing synaptic transmission under basil conditions (Burrone and Murthy, 2003; Turrigiano and Nelson, 2004). It is for these two reasons that it is important to think about the *Lis1* +/- mutant SC/CA1 synapse in a state of low probability of release, even though there are more spontaneous glutamatergic events.

Understanding the source of hyperexcitability in the *Lis1* +/- mutant leads to an exciting new way to think about treating lissencephaly, and possibly other models of cortical malformation and epilepsy. By focusing on the excitatory system and specifically reducing calcium entry in glutamatergic synapses, we believe that a successful treatment strategy may be developed. As discussed previously (Chapter One), the majority of antiepileptic drugs target the inhibitory system. These drugs are focused on enhancing inhibition and thus lowering excitability. Epileptic syndromes associated with a brain malformation are often resistant to the standard antiepileptic drugs (Jacobs et al., 1999; Smyth et al., 2002). Because our group has previously shown an increase in the inhibitory drive of the *Lis1* +/- mutants, it follows that trying to increase an already elevated system may not be effective. We now know that these mice have elevated glutamatergic transmission and it is, at least largely, due to an increase in presynaptic glutamatergic vesicle number. Reducing Ca^{2+} entry successfully reduced PPF to WT levels. We propose that non-surgical treatment for this disorder focus on reducing

excitatory transmission directly, either through existing experimental drugs (Löscher and Schmidt, 2006) and/or through the development of new drugs that reduce glutamatergic vesicular release.

Figure 1

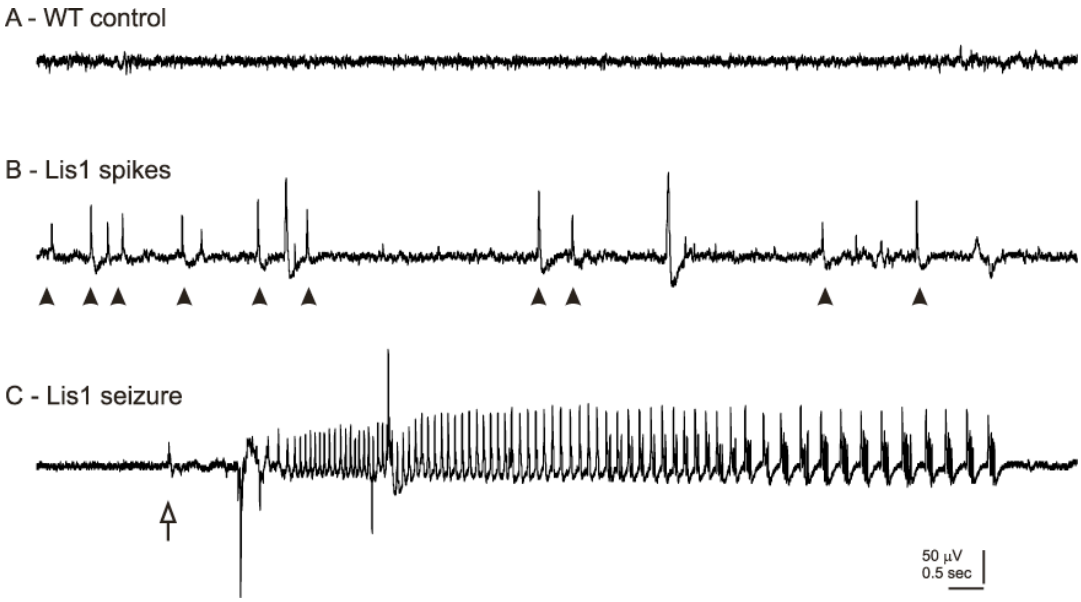

Figure 1: EEG activity recorded from scalp electrodes in freely moving mice. (A) Typical baseline electrographic activity in a *Lis1*$^{+/+}$ control mouse (n = 4). (B) Cortical spikes (arrowheads) recorded in a *Lis1*$^{+/-}$ mouse (n = 6). This pattern of electrographic activity was observed in 100% of *Lis1* +/- mutant mice. (B) Spontaneous electrographic seizure defined by the presence of polyspikes or sharp high-amplitude spiking lasting over 10 sec in duration. This pattern of electrographic activity was observed in 33% of *Lis1* +/- mutant mice.

Figure 2

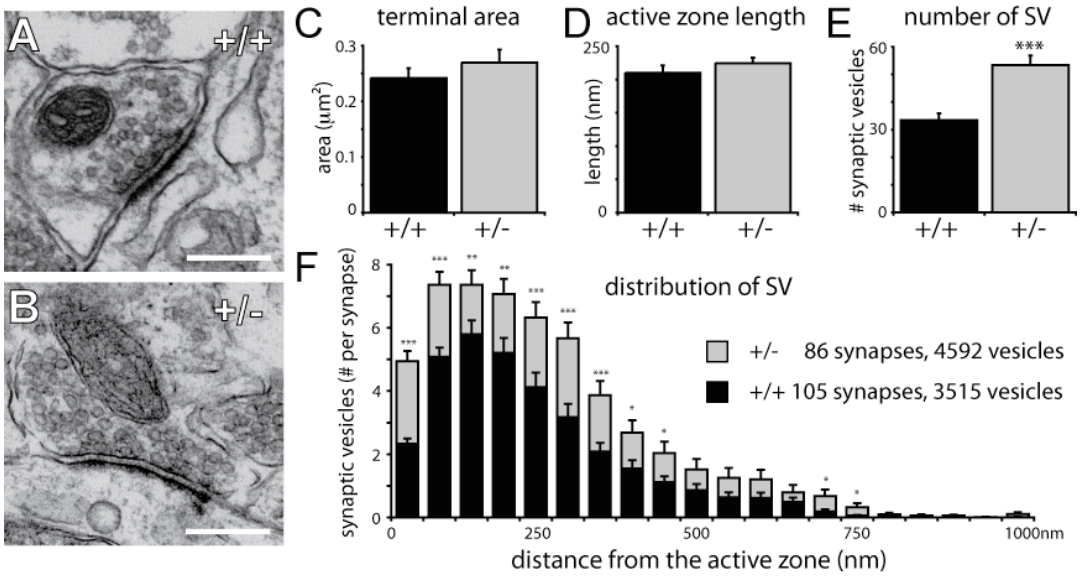
A
+/+
B
+/-
C
terminal area
area (µm²)
0.3
0.2
0.1
0
+/+
+/-
D
active zone length
length (nm)
250
0
+/+
+/-
E
number of SV
synaptic vesicles
60
30
0
***
+/+
+/-
F
distribution of SV
synaptic vesicles (# per synapse)
+/- 86 synapses, 4592 vesicles
+/+ 105 synapses, 3515 vesicles
0
250
500
750
1000nm
distance from the active zone (nm)

Figure 2: Ultrastructural analysis of *Lis1 +/-* mutant SC-CA1 synapses shows an increase in docked and total vesicle number without a change in terminal area or active zone length. Typical electron micrographs of asymmetric, SC-CA1 synapses from WT (A) and *Lis1* +/- mutant (B) littermates (Scale bar, 250nm). Micrographs were selected for analysis if the presynaptic terminal was intact and the postsynaptic density and synaptic cleft were discernable as asymmetric. An investigator blind to the genotype analyzed the micrographs. C) The terminal area is comparable between WT (0.24 ± 0.02 μm^2) and *Lis1* +/- mutants (0.27 ± 0.02 μm^2). D) The active zone length is comparable between WT (210 ± 11 nm) and *Lis1*+/- mutants (224 ± 8 nm). E) The total number of synaptic vesicles is significantly higher in *Lis1* +/- mutants (53 ± 3) than in WT littermates (33 ± 3). F) The distribution of synaptic vesicles relative to the active zone shows that there are significantly more docked vesicles (defined as being within 50nm of the postsynaptic density) in *Lis1* +/- mutants (4.9 ± 0.3) than WT littermates (2.3 ± 0.2). WT: black bars; 2 animals, 86 synapses. *Lis1* +/- mutants: gray bars; 3 animals, 105 synapses. Error is expressed as the standard deviation of the mean (SEM). Significance was calculated using two tailed, unpaired t-tests (* $p \leq 0.05$, ** $p \leq 0.01$, *** $p \leq 0.001$).

Figure 3

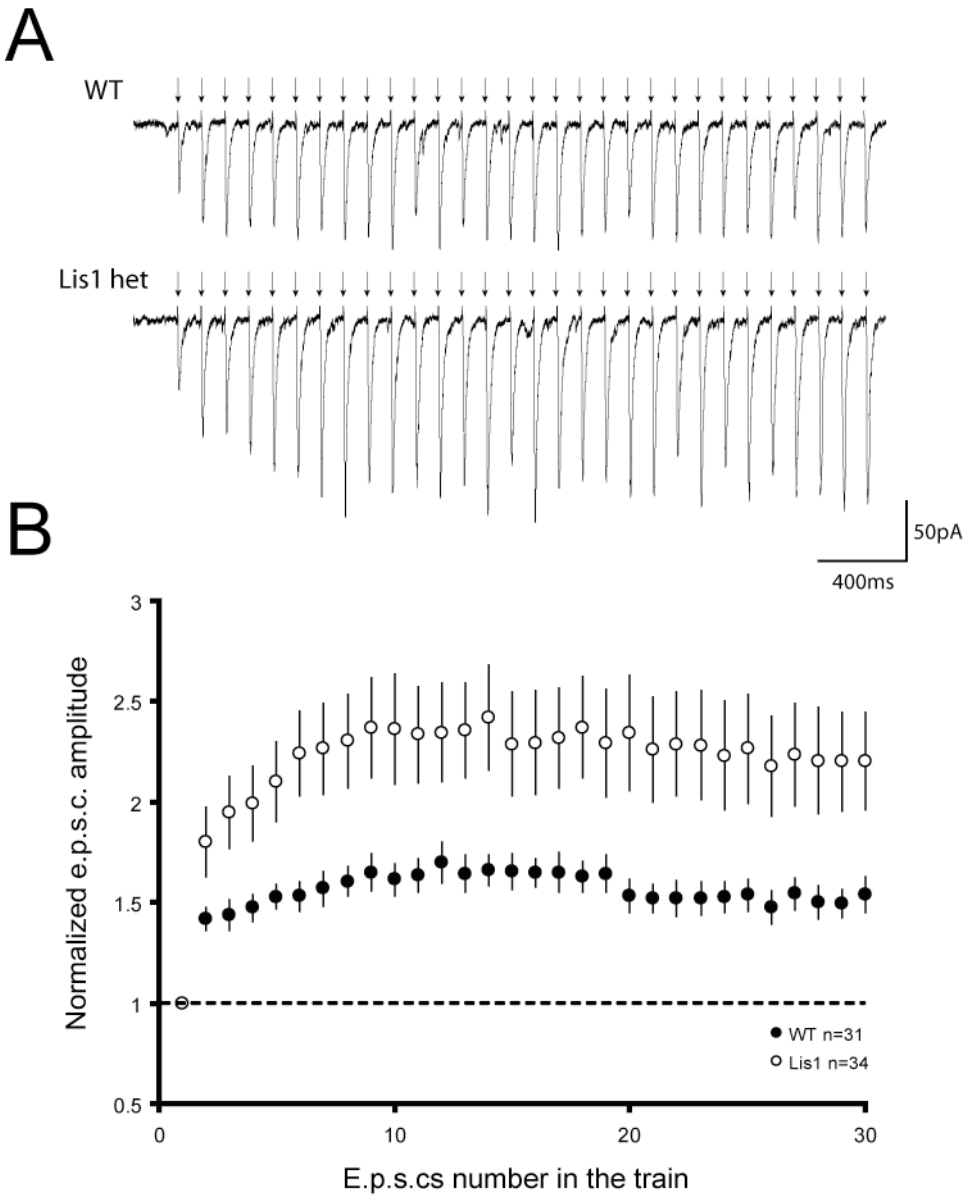
A
WT
Lis1 het
50pA
400ms
B
Normalized e.p.s.c. amplitude
3
2.5
2
1.5
1
0.5
0
10
20
30
E.p.s.cs number in the train
WT n=31
Lis1 n=34

Figure 3: Vesicle recycling and synaptic enhancement in *Lis1 +/-* mutants. A) Excitatory postsynaptic currents (EPSCs) recorded from a CA1 pyramidal cell in response to a 3 second, 10 Hz (every 100 ms) stimulation of the Shaffer collateral tract. The top trace is from a WT control and the bottom trace is from a *Lis1* +/- mutant. Arrows indicate stimulus events. B) EPSCs plotted from WT (closed circles; 8 animals, 31 slices) and *Lis1* +/- mutants (open circles; 9 animals, 34 slices). Three trials were taken for each cell and averaged together before normalization. EPSC amplitude was normalized to the first response in the train. *Lis1* +/- mutant and WT responses were significantly different ($p < 0.05$, two tailed, unpaired t-test) from the second pulse through to the end of the train. Error is graphed as the SEM.

Figure 4

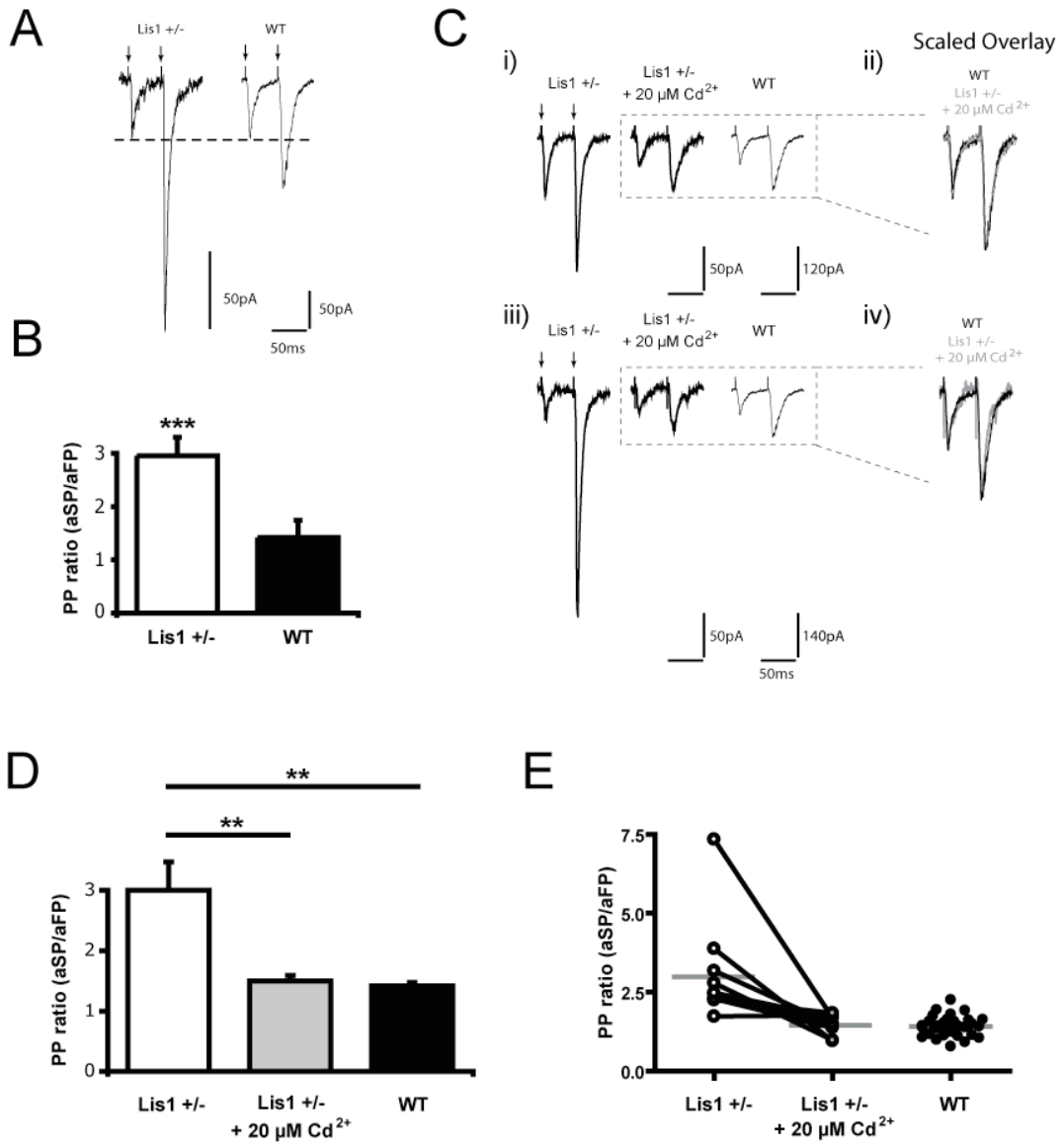
A
Lis1 +/-
WT
50pA
50pA
50ms
B
***
PP ratio (aSP/aFP)
3
2
1
0
Lis1 +/-
WT
C
i)
Lis1 +/-
Lis1 +/-
+ 20 µM Cd2+
WT
ii)
Scaled Overlay
WT
Lis1 +/-
+ 20 µM Cd2+
50pA
120pA
iii)
Lis1 +/-
Lis1 +/-
+ 20 µM Cd2+
WT
iv)
WT
Lis1 +/-
+ 20 µM Cd2+
50pA
140pA
50ms
D
**
**
PP ratio (aSP/aFP)
3
2
1
0
Lis1 +/-
Lis1 +/-
+ 20 µM Cd2+
WT
E
PP ratio (aSP/aFP)
7.5
5.0
2.5
0.0
Lis1 +/-
Lis1 +/-
+ 20 µM Cd2+
WT

Figure 4: Paired pulse facilitation (PPF) in CA1 pyramidal cells is enhanced in *Lis1* +/- mutants. The paired pulse ratio (PPR, second pulse divided by the first pulse) in *Lis1* +/- mutants is brought to WT levels with reduced calcium entry. A) Representative traces of PPF (50 ms, arrows mark stimulus events) in a *Lis1* +/- mutant and WT animal. Traces were scaled to the first response (scale bars: vertical, 50 pA; horizontal, 50ms). B) *Lis1* +/- mutants have a significantly larger PPR (3.0 ± 0.3; 6 animals, 29 cells) than WT littermates (1.4 ± 0.06; 8 animals, 31 cells). $p < 0.0001$; two tailed, unpaired t-test with Welch's correction (equal variances are not assumed). C) Limiting calcium entry with a low level of Cd^{2+}, in the extracellular bath, reduces the PPR in *Lis1* +/- animals to WT levels. i) Example traces of a *Lis1* +/- mutant cell before and after bath application of Cd^{2+} (20 μM). For comparison, a typical trace from a WT cell is shown; scaled to match the response to the first pulse (scale bars: vertical, 50 pA for *Lis1* +/-, 120 pA for WT; horizontal, 50 ms). ii) A scaled overlay of the same traces boxed in (i) on the left (*Lis1* +/- in 20 μM Cd^{2+} and WT in 0 μM Cd^{2+}). iii) Traces from the most extreme example in this data set where the PPR for the *Lis1* +/- mutant cell was 7.3 in 0 μM Cd^{2+} and near WT levels in 20 μM Cd^{2+} (scale bars: vertical, 50 pA for *Lis1* +/-, 140 pA for WT; horizontal, 50 ms). iv) A scaled overlay from the boxed traces in (iii) on the left. The same WT cell was used in comparison with the more typical example and the most extreme example from *Lis1* +/- mutants. D) The means of the 11 *Lis1* +/- cells tested in 0 and 20 μM Cd^{2+}. *Lis1* +/- mutant cells recorded in 0 μM Cd^{2+} have a significantly higher PPR (3.0 ± 0.5, 2 animals, 11 cells) than the same *Lis1* +/- mutants cells in 20 μM Cd^{2+} (1.5 ± 0.1) and WT littermates recorded in 0 μM Cd^{2+} (1.4 ± 0.06; 8 animals, 31

cells). For *Lis1* +/- 0 μM Cd^{2+} vs. *Lis1* +/- 20 μM Cd^{2+}: $p = 0.002$, Wilcoxon matched pairs test. For *Lis1* +/- 0 μM Cd^{2+} vs. WT in 0 μM Cd^{2+}: $p < 0.007$, two tailed, unpaired t-test with Welch's correction. There is no significant difference between the PPR of *Lis1* +/- mutant cells recorded in 20 μM Cd^{2+} and the PPR of WT cells recorded 0 μM Cd^{2+}. E) The results for all cells in (D) are shown. Circles represent the mean for individual cells and gray dotted lines represent the mean for each condition tested.

EPILOGUE

In this thesis I present evidence for a previously unappreciated role of Lis1 at the synapse. These data provide both a reasonable molecular explanation for seizure generation in a model of cortical malformation and a potential target for controlling this generation. It is my hope that this work spurs an examination of how we, as a field, think about cortical malformations.

In Chapter One I examined the basic components of the excitatory system in the hippocampus of the *Lis1* +/- mutant. I found that the primary glutamatergic receptors and transporters were present and, at least at a gross level, were present at comparable levels. Even though the CA1 pyramidal cells are dispersed in *Lis1* +/- mutants, they are integrated into the circuit, and electrophysiologically are indistinguishable from WT cells. However, glutamatergic input onto these cells is nearly doubled in *Lis1* +/- mutants. It is interesting to note that not all, but a large portion of that increased input is due to spontaneous release.

The level of spontaneous release is related to both P (the probability of fusion, ie. the probability of a given vesicle being released) and n (the number of release sites, which is frequently simplified to mean the number of synapses but is in fact the total number of release sites at those synapses). P is affected by changes the in release machinery whereas n is affected by changes in the number of synapses and/or the number of docked vesicles at those synapses. In Chapter Two, I showed that the total number of

vesicles, and specifically the number of docked vesicles, is increased in *Lis1* +/- mutant mice. So it is likely that the increase in spontaneous release is due to an increase in n.

In Chapter Two I also showed that short-term synaptic plasticity is enhanced in *Lis1* +/- mutants and that this enhancement can be rescued by limiting calcium entry. Since this enhancement may underlie hyperexcitability in these mice, this raises an exciting possibility for a non-surgical treatment strategy. This strategy would be to limit glutamatergic release directly instead of the more traditional, indirect method of enhancing inhibition. Gabapentin and pregabalin both inhibit presynaptic calcium channels and may be able to reduce excitability and seizures in *Lis1* +/- mutants. Levetiracetam may also work by inhibiting release of glutamatergic vesicles (reviewed in Löscher and Schmidt, 2006).

In this thesis I have shown that the number of vesicles is increased in *Lis1* +/- mutants; however, I have not ruled out that there could also be an increase in the number of synapses. I am able to recommend three places to start: 1) using a laser setup (described in Shao and Dudek, 2004) one could map the excitatory region of a given CA1 pyramidal cell and potentially show an enlarged area of excitation; 2) using GFP or YFP mice crossed to the *Lis1* mice (we used the m-line from Feng et al., 2000) one could look at neuronal connectivity and spines and hope to uncover either aberrant connectivity (e.g. recurrent CA1 pyramidal cell connectivity) or an increase in spine density; and finally, 3) using high throughput electron microscopy (currently being developed at the Center For Brain Science at Harvard University) one could reconstruct entire sections of the *Lis1* +/- mutant brain and with enough patience (read: graduate years), hopefully, find all sorts of interesting defects.

This mutant also presents an opportunity to reexamine our assumptions about basic synaptic physiology in the hippocampus. With a short, careful study one could show that the relationship between paired pulse facilitation (PPF) and the probability of release is not a simple inverse relationship. Upon close inspection of the original data (discussed in Chapter Two), I have come to believe that experimenters have been looking at a ceiling effect and, in fact, the *Lis1* +/- mutant would conform to those specific expectations if pushed to that ceiling. By recording PPF in a wide range of Ca2+ concentrations for both the *Lis1* +/- mutant and WT, one could show that the relationship between PPF and release probability is similar, while the dynamic range is either enlarged or shifted in *Lis1* +/- mutants. Another set of potentially fruitful experiments involves imaging vesicular release and recycling with FM143 (or equivalent) dye in dissociated hippocampal cultures from *Lis1* +/- mutants. Along those lines, one could also look at how fast vesicles accumulate by inhibiting *Lis1* function over shorter time periods (perhaps with RNAi as in Tsai et al., 2005) in the same system.

Finally, this thesis raises the possibility that short-term plasticity and/or vesicular release are altered in other models where an increase in excitatory drive has been reported (Simmons et al., 1997; Esclapez et al., 1999; Shao and Dudek, 2004; Jacobs and Prince, 2005).

Due to the dramatic nature of the neuronal disorganization in lissencephaly, it comes as no surprise that the majority of work on *Lis1* has been focused on its role in neuronal migration. Indeed, my original hypotheses were all based on the notion that the

disorganization itself must somehow lead to seizure generation.[2] As with most scientific writing I have not presented the experiments in the order in which they were performed. I also regret to admit that I was not nearly as prescient as I have lead you, the reader, to believe. There was no greater surprise than my own when I discovered that the number of vesicles was greater in *Lis1* +/- mutants. Fortunately, the scientific process affords the experimenter the luxury of reexamining hypotheses and letting the data guide interpretation instead of interpretation guiding the data. I relay this to send hope (and a warning) to anyone mired in the depths of scientific minutia. What I found in the end was not at all what I expected in the beginning and the most obvious defects were, in fact, misleading. So I leave you with this to ponder: Don't get distracted by the forest; sometimes the trees are more important than you think.

[2] It was only with lengthy and painful failure to prove this that I turned to other avenues of experimentation.

REFERENCES

Asztely, F., Xiao, M. Y., and Gustafsson, B. (1996). Long-term potentiation and paired-pulse facilitation in the hippocampal CA1 region. Neuroreport *7*, 1609-1612.

Atwood, H. L. (1976). Organization and synaptic physiology of crustacean neuromuscular systems. Progress in neurobiology *7*, 291-391.

Babb, T. L., Ying, Z., Hadam, J., and Penrod, C. (1998). Glutamate receptor mechanisms in human epileptic dysplastic cortex. Epilepsy research *32*, 24-33.

Bandyopadhyay, S., and Hablitz, J. J. (2006). NR2B antagonists restrict spatiotemporal spread of activity in a rat model of cortical dysplasia. Epilepsy research *72*, 127-139.

Barallobre, M. J., Del Río, J. A., Alcántara, S., Borrell, V., Aguado, F., Ruiz, M., Carmona, M. A., Martín, M., Fabre, M., Yuste, R., Tessier-Lavigne, M., and Soriano, E. (2000). Aberrant development of hippocampal circuits and altered neural activity in netrin 1-deficient mice. Development (Cambridge, England) *127*, 4797-4810.

Barkovich, A. J., Koch, T. K., and Carrol, C. L. (1991). The spectrum of lissencephaly:

report of ten patients analyzed by magnetic resonance imaging. Annals of neurology *30*, 139-146.

Burrone, J., and Murthy, V. N. (2003). Synaptic gain control and homeostasis. Current opinion in neurobiology *13*, 560-567.

Calcagnotto, M. E., and Baraban, S. C. (2005). Prolonged NMDA-mediated responses, altered ifenprodil sensitivity, and epileptiform-like events in the malformed hippocampus of methylazoxymethanol exposed rats. Journal of neurophysiology *94*, 153-162.

Castro, P. A., Cooper, E. C., Lowenstein, D. H., and Baraban, S. C. (2001). Hippocampal heterotopia lack functional Kv4.2 potassium channels in the methylazoxymethanol model of cortical malformations and epilepsy. The Journal of neuroscience : the official journal of the Society for Neuroscience *21*, 6626-6634.

Cepeda, C., André, V. M., Levine, M. S., Salamon, N., Miyata, H., Vinters, H. V., and Mathern, G. W. (2006). Epileptogenesis in pediatric cortical dysplasia: the dysmature cerebral developmental hypothesis. Epilepsy & behavior : E&B *9*, 219-235.

Cheng, H. J., Bagri, A., Yaron, A., Stein, E., Pleasure, S. J., and Tessier-Lavigne, M.

(2001). Plexin-A3 mediates semaphorin signaling and regulates the development of hippocampal axonal projections. Neuron *32*, 249-263.

Cohen-Gadol, A. A., Ozduman, K., Bronen, R. A., Kim, J. H., and Spencer, D. D. (2004). Long-term outcome after epilepsy surgery for focal cortical dysplasia. Journal of neurosurgery *101*, 55-65.

Colacitti, C., Sancini, G., DeBiasi, S., Franceschetti, S., Caputi, A., Frassoni, C., Cattabeni, F., Avanzini, G., Spreafico, R., Di Luca, M., and Battaglia, G. (1999). Prenatal methylazoxymethanol treatment in rats produces brain abnormalities with morphological similarities to human developmental brain dysgeneses. Journal of neuropathology and experimental neurology *58*, 92-106.

Crino, P. B., Duhaime, A. C., Baltuch, G., and White, R. (2001). Differential expression of glutamate and GABA-A receptor subunit mRNA in cortical dysplasia. Neurology *56*, 906-913.

DeFazio, R. A., and Hablitz, J. J. (2000). Alterations in NMDA receptors in a rat model of cortical dysplasia. Journal of neurophysiology *83*, 315-321.

Dobyns, W. B., and Truwit, C. L. (1995). Lissencephaly and other malformations of cortical development: 1995 update. Neuropediatrics *26*, 132-147.

Doussau, F., Clabecq, A., Henry, J. P., Darchen, F., and Poulain, B. (1998). Calcium-dependent regulation of rab3 in short-term plasticity. The Journal of neuroscience : the official journal of the Society for Neuroscience *18*, 3147-3157.

Drakew, A., Deller, T., Heimrich, B., Gebhardt, C., Del Turco, D., Tielsch, A., Förster, E., Herz, J., and Frotscher, M. (2002). Dentate granule cells in reeler mutants and VLDLR and ApoER2 knockout mice. Experimental neurology *176*, 12-24.

Dudel, J. (1990). Inhibition of Ca2+ inflow at nerve terminals of frog muscle blocks facilitation while phasic transmitter release is still considerable. Pflügers Archiv : European journal of physiology *415*, 566-574.

Efimov, V. P., and Morris, N. R. (2000). The LIS1-related NUDF protein of Aspergillus nidulans interacts with the coiled-coil domain of the NUDE/RO11 protein. The Journal of cell biology *150*, 681-688.

Esclapez, M., Hirsch, J. C., Ben-Ari, Y., and Bernard, C. (1999). Newly formed excitatory pathways provide a substrate for hyperexcitability in experimental temporal lobe epilepsy. The Journal of comparative neurology *408*, 449-460.

Faulkner, N. E., Dujardin, D. L., Tai, C. Y., Vaughan, K. T., O'Connell, C. B., Wang, Y., and Vallee, R. B. (2000). A role for the lissencephaly gene LIS1 in mitosis and cytoplasmic dynein function. Nature cell biology *2*, 784-791.

Feng, G., Mellor, R. H., Bernstein, M., Keller-Peck, C., Nguyen, Q. T., Wallace, M., Nerbonne, J. M., Lichtman, J. W., and Sanes, J. R. (2000). Imaging neuronal subsets in transgenic mice expressing multiple spectral variants of GFP. Neuron *28*, 41-51.

Fisher, S. A., Fischer, T. M., and Carew, T. J. (1997). Multiple overlapping processes underlying short-term synaptic enhancement. Trends in neurosciences *20*, 170-177.

Fleck, M. W., Hirotsune, S., Gambello, M. J., and al., e. (2000). Hippocampal abnormalities and enhanced excitability in a murine model of human lissencephaly. J Neurosci *20*, 2439-2450.

Geppert, M., Bolshakov, V. Y., Siegelbaum, S. A., Takei, K., De Camilli, P., Hammer, R. E., and Südhof, T. C. (1994). The role of Rab3A in neurotransmitter release. Nature *369*, 493-497.

Hagemann, G., Kluska, M. M., Redecker, C., Luhmann, H. J., and Witte, O. W. (2003). Distribution of glutamate receptor subunits in experimentally induced cortical malformations. Neuroscience *117*, 991-1002.

Harrington, E. P., Möddel, G., Najm, I. M., and Baraban, S. C. (2007). Altered glutamate

receptor - transporter expression and spontaneous seizures in rats exposed to methylazoxymethanol in utero. Epilepsia *48*, 158-168.

Hirotsune, S., Fleck, M. W., Gambello, M. J., Bix, G. J., Chen, A., Clark, G. D., Ledbetter, D. H., McBain, C. J., and Wynshaw-Boris, A. (1998). Graded reduction of Pafah1b1 (Lis1) activity results in neuronal migration defects and early embryonic lethality. Nature genetics *19*, 333-339.

Isaac, J. T., Nicoll, R. A., and Malenka, R. C. (1995). Evidence for silent synapses: implications for the expression of LTP. Neuron *15*, 427-434.

Jacobs, K. M., Kharazia, V. N., and Prince, D. A. (1999). Mechanisms underlying epileptogenesis in cortical malformations. Epilepsy research *36*, 165-188.

Jacobs, K. M., and Prince, D. A. (2005). Excitatory and inhibitory postsynaptic currents in a rat model of epileptogenic microgyria. Journal of neurophysiology *93*, 687-696.

(2007). Electron Microscopy: Methods and Protocols Humana Press).

Jones, D. L., and Baraban, S. C. (2007). Characterization of inhibitory circuits in the malformed hippocampus of lis1 mutant mice. Journal of neurophysiology *98*, 2737-2746.

Katz, B. (1962). The Croonian Lecture: The Transmission of Impulses from Nerve to Muscle, and the Subcellular Unit of …. Proceedings of the Royal Society of London. Series B

Kawauchi, T., and Hoshino, M. (2008). Molecular pathways regulating cytoskeletal organization and morphological changes in migrating neurons. Developmental neuroscience *30*, 36-46.

Kerjan, Gleeson (2007). Genetic mechanisms underlying abnormal neuronal migration in classical lissencephaly. Trends Genet .

Kral, T., Clusmann, H., Blümcke, I., Fimmers, R., Ostertun, B., Kurthen, M., and Schramm, J. (2003). Outcome of epilepsy surgery in focal cortical dysplasia. Journal of neurology, neurosurgery, and psychiatry *74*, 183-188.

Kreitzer, A. C., and Regehr, W. G. (2000). Modulation of transmission during trains at a cerebellar synapse. The Journal of neuroscience : the official journal of the Society for Neuroscience *20*, 1348-1357.

Kushner, S. A., Elgersma, Y., Murphy, G. G., Jaarsma, D., van Woerden, G. M., Hojjati, M. R., Cui, Y., LeBoutillier, J. C., Marrone, D. F., Choi, E. S., De Zeeuw, C. I., Petit, T. L., Pozzo-Miller, L., and Silva, A. J. (2005). Modulation of presynaptic

plasticity and learning by the H-ras/extracellular signal-regulated kinase/synapsin I signaling pathway. The Journal of neuroscience : the official journal of the Society for Neuroscience *25*, 9721-9734.

Lai, C., Lin, X., Chandran, J., Shim, H., Yang, W.-J., and Cai, H. (2007). The G59S mutation in p150(glued) causes dysfunction of dynactin in mice. The Journal of neuroscience : the official journal of the Society for Neuroscience *27*, 13982-13990.

Li, H., and Prince, D. A. (2002). Synaptic activity in chronically injured, epileptogenic sensory-motor neocortex. Journal of neurophysiology *88*, 2-12.

Li, J. Y., Pfister, K. K., Brady, S. T., and Dahlström, A. (2000). Cytoplasmic dynein conversion at a crush injury in rat peripheral axons. Journal of neuroscience research *61*, 151-161.

Löscher, W., and Schmidt, D. (2006). New Horizons in the development of antiepileptic drugs: Innovative strategies. Epilepsy research *69*, 183-272.

Manabe, T., Wyllie, D. J., Perkel, D. J., and Nicoll, R. A. (1993). Modulation of synaptic transmission and long-term potentiation: effects on paired pulse facilitation and EPSC variance in the CA1 region of the hippocampus. Journal of neurophysiology *70*, 1451-1459.

Mathern, G. W., Pretorius, J. K., Mendoza, D., Lozada, A., Leite, J. P., Chimelli, L., Fried, I., Sakamoto, A. C., Assirati, J. A., and Adelson, P. D. (1998). Increased hippocampal AMPA and NMDA receptor subunit immunoreactivity in temporal lobe epilepsy patients. Journal of neuropathology and experimental neurology *57*, 615-634.

Mizielinska, S. M. (2007). Ion channels in epilepsy. Biochemical Society transactions *35*, 1077-1079.

Morris, N. R., Efimov, V. P., and Xiang, X. (1998). Nuclear migration, nucleokinesis and lissencephaly. Trends in cell biology *8*, 467-470.

Niethammer, M., Smith, D. S., Ayala, R., Peng, J., Ko, J., Lee, M. S., Morabito, M., and Tsai, L. H. (2000). NUDEL is a novel Cdk5 substrate that associates with LIS1 and cytoplasmic dynein. Neuron *28*, 697-711.

Patrylo, P. R., and Willingham, A. (2007). Anatomic and electrophysiologic evidence for a proconvulsive circuit in the dentate gyrus of reeler mutant mice, an animal model of diffuse cortical malformation. Developmental neuroscience *29*, 73-83.

Paylor, R., Hirotsune, S., Gambello, M. J., Yuva-Paylor, L., Crawley, J. N., and Wynshaw-Boris, A. (1999). Impaired learning and motor behavior in

heterozygous Pafah1b1 (Lis1) mutant mice. Learning & memory (Cold Spring Harbor, NY) *6*, 521-537.

Perez, Y., Morin, F., Beaulieu, C., and Lacaille, J. C. (1996). Axonal sprouting of CA1 pyramidal cells in hyperexcitable hippocampal slices of kainate-treated rats. The European journal of neuroscience *8*, 736-748.

Perrin, F. E., and Stoeckli, E. T. (2000). Use of lipophilic dyes in studies of axonal pathfinding in vivo. Microscopy research and technique *48*, 25-31.

Reiner, O., Cahana, A., Escamez, T., and Martinez, S. (2002). LIS1-no more no less. Molecular psychiatry *7*, 12-16.

Reiner, O., Carrozzo, R., Shen, Y., Wehnert, M., Faustinella, F., Dobyns, W. B., Caskey, C. T., and Ledbetter, D. H. (1993). Isolation of a Miller-Dieker lissencephaly gene containing G protein beta-subunit-like repeats. Nature *364*, 717-721.

Ritter, L. M., Vazquez, D. M., and Meador-Woodruff, J. H. (2002). Ontogeny of ionotropic glutamate receptor subunit expression in the rat hippocampus. Brain research Developmental brain research *139*, 227-236.

Rizzoli, S. O., and Betz, W. J. (2005). Synaptic vesicle pools. Nature reviews Neuroscience *6*, 57-69.

Rogers, S. W., Hughes, T. E., Hollmann, M., Gasic, G. P., Deneris, E. S., and Heinemann, S. (1991). The characterization and localization of the glutamate receptor subunit GluR1 in the rat brain. The Journal of neuroscience : the official journal of the Society for Neuroscience *11*, 2713-2724.

Rothstein, J. D., Dykes-Hoberg, M., Pardo, C. A., Bristol, L. A., Jin, L., Kuncl, R. W., Kanai, Y., Hediger, M. A., Wang, Y., Schielke, J. P., and Welty, D. F. (1996). Knockout of glutamate transporters reveals a major role for astroglial transport in excitotoxicity and clearance of glutamate. Neuron *16*, 675-686.

Rothstein, J. D., Jin, L., Dykes-Hoberg, M., and Kuncl, R. W. (1993). Chronic inhibition of glutamate uptake produces a model of slow neurotoxicity. Proceedings of the National Academy of Sciences of the United States of America *90*, 6591-6595.

Santos, M., Li, H., and Voglmaier, S. (2008). Synaptic vesicle protein trafficking at the glutamate synapse. Neuroscience .

Sapir, T., Elbaum, M., and Reiner, O. (1997). Reduction of microtubule catastrophe events by LIS1, platelet-activating factor acetylhydrolase …. The EMBO Journal

Sasaki, S., Shionoya, A., Ishida, M., Gambello, M. J., Yingling, J., Wynshaw-Boris, A., and Hirotsune, S. (2000). A LIS1/NUDEL/cytoplasmic dynein heavy chain

complex in the developing and adult nervous system. Neuron *28*, 681-696.

Schwartzkroin, P. A., and Walsh, C. A. (2000). Cortical malformations and epilepsy. Mental retardation and developmental disabilities research reviews *6*, 268-280.

Shao, L.-R., and Dudek, F. E. (2004). Increased excitatory synaptic activity and local connectivity of hippocampal CA1 pyramidal cells in rats with kainate-induced epilepsy. Journal of neurophysiology *92*, 1366-1373.

Simmons, M. L., Terman, G. W., and Chavkin, C. (1997). Spontaneous excitatory currents and kappa-opioid receptor inhibition in dentate gyrus are increased in the rat pilocarpine model of temporal lobe epilepsy. Journal of neurophysiology *78*, 1860-1868.

Smith, B. N., and Dudek, F. E. (2002). Network interactions mediated by new excitatory connections between CA1 pyramidal cells in rats with kainate-induced epilepsy. Journal of neurophysiology *87*, 1655-1658.

Smith, C. (1999). A persistent activity-dependent facilitation in chromaffin cells is caused by Ca2+ activation of protein kinase C. The Journal of neuroscience : the official journal of the Society for Neuroscience *19*, 589-598.

Smyth, M. D., Barbaro, N. M., and Baraban, S. C. (2002). Effects of antiepileptic drugs

on induced epileptiform activity in a rat model of dysplasia. Epilepsy research *50*, 251-264.

Srinivasan, G., Kim, J. H., and von Gersdorff, H. (2008). The pool of fast releasing vesicles is augmented by myosin light chain kinase inhibition at the calyx of Held synapse. Journal of neurophysiology *99*, 1810-1824.

Swann, J. W., and Hablitz, J. J. (2000). Cellular abnormalities and synaptic plasticity in seizure disorders of the immature nervous system. Mental retardation and developmental disabilities research reviews *6*, 258-267.

Toonen, R. F. G., Wierda, K., Sons, M. S., de Wit, H., Cornelisse, L. N., Brussaard, A., Plomp, J. J., and Verhage, M. (2006). Munc18-1 expression levels control synapse recovery by regulating readily releasable pool size. Proceedings of the National Academy of Sciences of the United States of America *103*, 18332-18337.

Tsai, J.-W., Chen, Y., Kriegstein, A. R., and Vallee, R. B. (2005). LIS1 RNA interference blocks neural stem cell division, morphogenesis, and motility at multiple stages. The Journal of cell biology *170*, 935-945.

Turrigiano, G. G., and Nelson, S. B. (2004). Homeostatic plasticity in the developing nervous system. Nature reviews Neuroscience *5*, 97-107.

Tyler, W. J., and Pozzo-Miller, L. D. (2001). BDNF enhances quantal neurotransmitter release and increases the number of docked vesicles at the active zones of hippocampal excitatory synapses. The Journal of neuroscience : the official journal of the Society for Neuroscience *21*, 4249-4258.

Valdés-Sánchez, L., Escámez, T., Echevarria, D., Ballesta, J. J., Tabarés-Seisdedos, R., Reiner, O., Martinez, S., and Geijo-Barrientos, E. (2007). Postnatal alterations of the inhibitory synaptic responses recorded from cortical pyramidal neurons in the Lis1/sLis1 mutant mouse. Molecular and cellular neurosciences *35*, 220-229.

Virmani, T., Ertunc, M., Sara, Y., Mozhayeva, M., and Kavalali, E. T. (2005). Phorbol esters target the activity-dependent recycling pool and spare spontaneous vesicle recycling. The Journal of neuroscience : the official journal of the Society for Neuroscience *25*, 10922-10929.

Wang, S., Hu, P., Wang, H.-L., Wang, M., Chen, J.-T., Tang, J.-L., and Ruan, D.-Y. (2008). Effects of Cd(2+) on AMPA receptor-mediated synaptic transmission in rat hippocampal CA1 area. Toxicology letters *176*, 215-222.

Wojtowicz, J. M., Marin, L., and Atwood, H. L. (1994). Activity-induced changes in synaptic release sites at the crayfish neuromuscular junction. The Journal of neuroscience : the official journal of the Society for Neuroscience *14*, 3688-3703.

Wolf, H. K., Buslei, R., Schmidt-Kastner, R., Schmidt-Kastner, P. K., Pietsch, T., Wiestler, O. D., and Blümcke, I. (1996). NeuN: a useful neuronal marker for diagnostic histopathology. The journal of histochemistry and cytochemistry : official journal of the Histochemistry Society *44*, 1167-1171.

Woodhams, P. L., and Terashima, T. (2000). Aberrant trajectory of entorhino-dentate axons in the mutant Shaking Rat Kawasaki: a Dil-labelling study. The European journal of neuroscience *12*, 2707-2720.

Wynshaw-Boris, A. (2007). Lissencephaly and LIS1: insights into the molecular mechanisms of neuronal migration and development. Clinical genetics *72*, 296-304.

Ying, Z., Babb, T. L., Comair, Y. G., Bingaman, W., Bushey, M., and Touhalisky, K. (1998). Induced expression of NMDAR2 proteins and differential expression of NMDAR1 splice variants in dysplastic neurons of human epileptic neocortex. Journal of neuropathology and experimental neurology *57*, 47-62.

Zengel, J. E., Lee, D. T., Sosa, M. A., and Mosier, D. R. (1993). Effects of calcium channel blockers on stimulation-induced changes in transmitter release at the frog neuromuscular junction. Synapse (New York, NY) *15*, 251-262.

Zengel, J. E., Sosa, M. A., and Poage, R. E. (1993). omega-Conotoxin reduces facilitation of transmitter release at the frog neuromuscular junction. Brain research *611*, 25-30.

Zsombok, A., and Jacobs, K. M. (2007). Postsynaptic currents prior to onset of epileptiform activity in rat microgyria. Journal of neurophysiology *98*, 178-186.

Zucker, R. S., and Regehr, W. G. (2002). Short-term synaptic plasticity. Annual review of physiology *64*, 355-405.

Library Release

Publishing Agreement

It is the policy of the University to encourage the distribution of all theses and dissertations. Copies of all UCSF theses and dissertations will be routed to the library via the Graduate Division. The library will make all theses and dissertations accessible to the public and will preserve these to the best of their abilities, in perpetuity.

Please sign the following statement:

I hereby grant permission to the Graduate Division of the University of California, San Francisco to release copies of my thesis or dissertation to the Campus Library to provide
access and preservation, in whole or in part, in perpetuity.

Author Signature

9/9/2008
Date